ABSTRACT

CONCENTRATION-DEPENDENT CYANIDE ACTION MONITORED USING SPECTRAL PHASOR ANALYSIS OF UV-EXCITED CELLULAR AUTOFLUORESCENCE

by Nazar Khalaf Mahan Al-Aayedi

Spectral phasor analysis on nanosecond-gated UV-excited cellular autofluorescence is being developed for the real-time monitoring of metabolism. Previous studies have shown that emission signals are primarily due to reduced nicotinamide adenine dinucleotide (NADH) forms, significant because NADH is used as a metabolic indicator and biomarker and because the various NADH forms respond diff erently to changes in mitochondrial function. Here we apply the monitoring technique to investigate the autofluorescence response of cellular suspensions to additions of cyanide, an inhibitor of cellular respiration. Using spectral phasor analysis to assess whether observed spectral changes are consistent with a two-state model, here we implement a spectral-phasor approach capable of measuring small shifts in NADH autofluorescence when using mitochondrial functional modifiers (cyanide and glucose). The ability of a spectral-phasor approach in detecting quantification of spectrum shape can be useful in the real-time, non-invasive detection of small diff erences between cellular metabolic responses.

# CONCENTRATION-DEPENDENT CYANIDE ACTION MONITORED USING SPECTRAL PHASOR ANALYSIS OF UV-EXCITED CELLULAR AUTOFLUORESCENCE

Thesis

Submitted to the

Faculty of Miami University

in partial fulfillment of

the requirements for the degree of

Master of Science

by

Nazar Khalaf Mahan Al-Aayedi

Miami University

Oxford, Ohio

2018

Advisor: Dr. Paul Urayama

Reader: Dr. Khalid Eid

Reader: Dr. Herbert Jaeger

This thesis titled

CONCENTRATION-DEPENDENT CYANIDE ACTION MONITORED USING SPECTRAL PHASOR ANALYSIS OF UV-EXCITED CELLULAR AUTOFLUORESCENCE

by

Nazar Khalaf Mahan Al-Aayedi

has been approved for publication by

The College Arts and Science

and

Department of Physics

_____

Dr. Paul Urayama, Advisor

_____

Dr. Khalid Eid, Reader

_____

Dr. Herbert Jaeger, Reader

# Table of Contents

# List of Tables

# List of Figures

**Fig 3.1.2.1:** Monitoring autofluorescence response to cyanide additions. In the figure, full gate data, spectrally integrated intensity versus time, and late gate data, spectrally time-gated autofluorescence, normalized to the intensity prior to chemical addition (cyanide). Autofluorescence spectra filled symbol (before cyanide addition) and open symbol (after cyanide addition). Similarly, figures are shown on the (left) full gate data and, on the (Right), late gate data for addition of 10mM, 1mM, 900μM, 700μM, 500μM, 250μM, 100μM and 50μM of cyanide.

**Fig 3.1.3.1:** Spectral phasor plots for different concentration of cyanide added. In all figures, full gate data are blue circles, and late-gate data are red squares. Each data point is a spectrally integrated intensity versus time, normalized to the intensity prior to chemical addition (Cyanide). Filled symbols are before cyanide addition and open symbols are after cyanide addition. Similarly, figures are shown on the (top) for addition of 10mM, 1mM, 900μM and 700μM cyanide. On the bottom, 500μM, 250μM, 100μM, and 50μM of cyanide.

**Fig 3.1.4.1:** Monitoring autofluorescence response to cyanide additions. In the figure, full gate data, spectrally integrated intensity versus time, and late gate data, spectrally time-gated autofluorescence, normalized to the intensity prior to chemical addition (Cyanide). Autofluorescence spectra filled symbol (before cyanide addition) and open symbol (after cyanide addition). Similarly, figures are shown on the (left) full gate data and on the (Right), late gate data for addition of 10mM, 1mM, 900μM, 700μM, 500μM, 250μM, 100μM and 50μM of cyanide.

**Fig 3.1.4.2:** Emission spectrum before and after addition of cyanide. The blue spectrum is before cyanide added and the red spectrum is after cyanide added.

**Fig 3.2.1.1:** Monitoring autofluorescence response to D-glucose and cyanide additions. In all figures, full gate data are blue circles, and late-gate data are red squares. Each data point is a spectrally integrated intensity versus time, normalized to the intensity prior to chemical addition (Cyanide). Filled symbols are before cyanide addition and open symbols are after cyanide addition. Similarly, figures are shown on the (top) for addition of 10mM, 1mM, 900μM and 700μM cyanide. On the bottom, 500μM, 250μM, 100μM, and 50μM of cyanide. In all experiments, 3mM D-glucose was added 15mins prior to adding cyanide.

spectrally time-gated autofluorescence, normalized to the intensity prior to chemical addition (Cyanide). Autofluorescence spectra filled symbol (before cyanide addition) and open symbol (after cyanide addition). Similarly, figures are shown on the (left) Nazar data. But, figures are shown on the (right) Madhu data.

## Abbreviations

**NADH :** Nicotinamide adenine dinucleotide

**$FADH_2$ :** Reduced flavin adenine dinucleotide

**KCN :** Potassium Cyanide

**PBS :** Phosphate buffered Saline

**ICCD :** Intensified charge-coupled Device

**POPOP:** 1,4-Bis(5-phemyl-2-oxazolyl) benzene

**9-CA :** 9-anthracenecarboxylic acid

# Dedication

This thesis is dedicated to my family and friends that have the source of inspiration and encouragement for me. They are always unconditional support of what I do, and I always would like to talk to them.

## Acknowledgements

Among many people who have helped me complete my thesis.

I would like to express my sincere gratitude my advisor, Dr. Paul Urayama, for providing me with this research and writing processes. I really appreciate with guidance and support throughout and helping in the analysis of the data.

I would also like to thank my committee members Dr. Khalid Eid, Dr. Karthik Vishwanath and Dr. Herbert Jaeger for their comments and suggestions during my prospectus.

I would like to say thankful my lab mates Gaire Madhu and Heidelman Martin for helping and providing ideas when I was having difficulty problems in this thesis.

# Chapter 1: Introduction

## 1.1 Cellular Respiration

Respiration is a known method of chemical energy production for cellular activity, which involves many biochemical processes like the reduction and oxidization of NADH (reduced nicotinamide adenine dinucleotide) and $FADH_2$ (reduced flavin adenine dinucleotide) [1].During the process, it produces carbon dioxide, water and energy as shown in the following net reaction $C_6H_{12}O_6$ (s) + $6O_2$ (g) → $6CO_2$ (g) + $6H_2O$ (l)+ heat. Energy production either utilizes the aerobic respiratory pathway or the fermentation pathway. The aerobic respiration pathway first breaks down glucose in the cytoplasm, and then in the mitochondria, $NAD^+$ is reduced to NADH (Krebs Cycle), and then in the mitochondrial membrane, NADH is oxidized to $NAD^+$ (electron transport chain), producing a proton gradient which ultimately produces ATP (adenosine triphosphate). Alternatively, ATP production can proceed through the fermentation pathway producing ethanol (in yeast) or in Lactic acid (humans) as bioproduct [1], [2]. However, the aerobic respiratory pathway is far more effective in producing ATP than the fermentation pathway. 38 ATP molecules can be made per each glucose molecule during cellular respiration (2 in glycolysis, 2 in the Krebs cycle, and about 34 in the electron transport system) while only 2 ATP molecules are produced in the fermentation pathway [2] (See figure 1.1.1).

Mitochondrial function plays a fundamental role in cell metabolism. Therefore, it is useful to study transitions from function and dysfunction. Due to the fact that (NADH\$NAD^+$) and ($FADH_2$\$FAD^+$) are sources of autofluorescence and that they play pivotal roles in reduction and oxidization in cellular respiration, allows for the noninvasive tracking of metabolic activity and the detection of mitochondrial dysfunction [3]. Using methods sensitive to changes in spectrum shape, we can study the change in proportions of free and bound NADH conformation because the free and protein-bound NADH have also a different lifetime. The time resolved measurement of fluoresce spectra provide addition al information to monitor metabolic responses related between spectrum shape change and time-resolved measurements of fluorescence about mitochondrial activities.

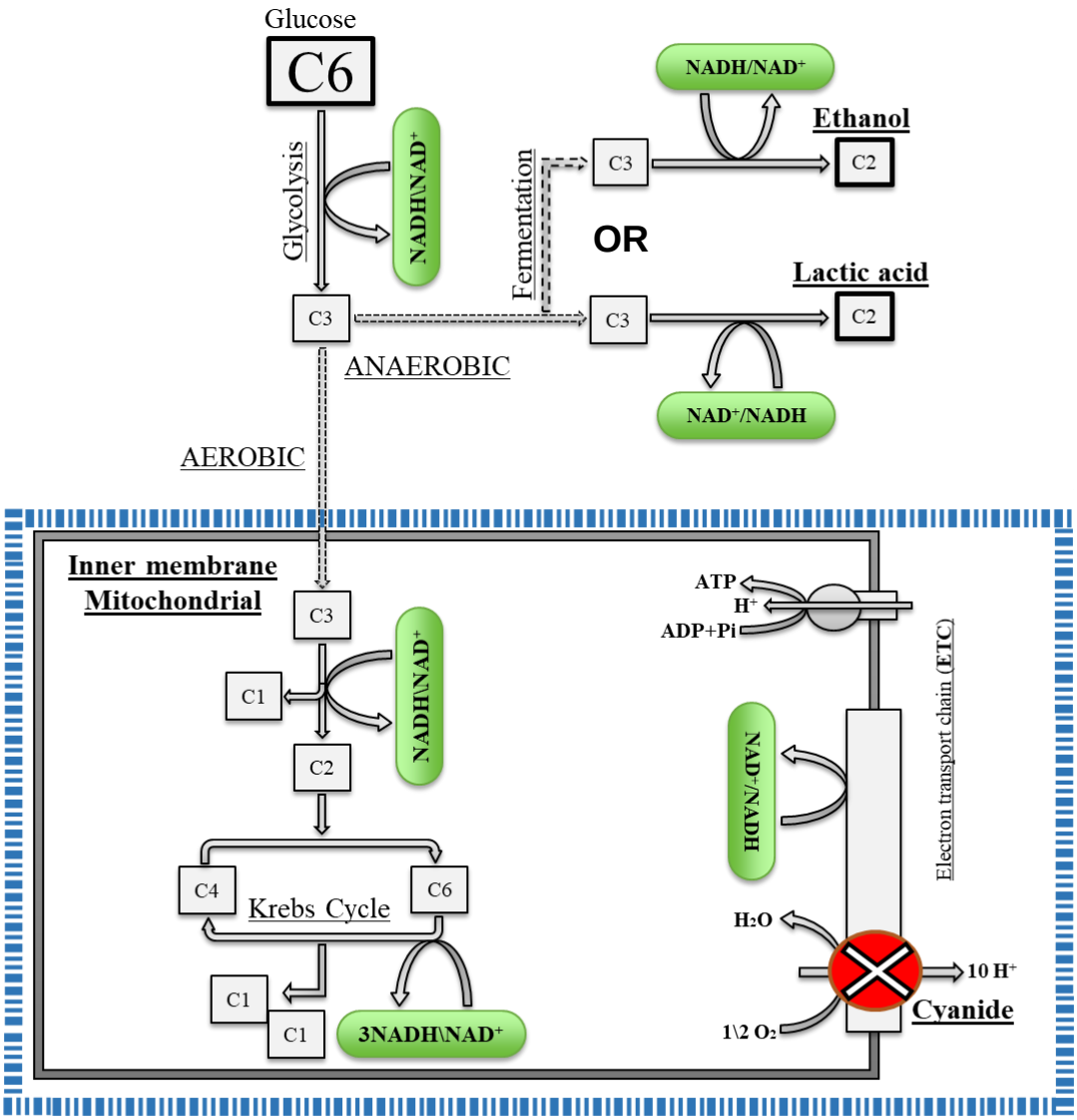


**Fig 1.1.1:** Cellular respiration showing the process with oxygen.

During glycolysis, which occurs in the cytoplasm of cells in all living organisms, one molecule of glucose is converted into two pyruvates, a three-carbon organic molecule, producing two ATP and two NADH molecules via reduction. The two pyruvates then cross the fermentation pathway then split into one two carbon molecule as the ethanol in yeast or carbon molecule as the lactic acid in humans[2]. In the aerobic pathway, the two pyruvates then cross the mitochondrial membrane into the mitochondria and both molecules are then split into two two-carbon molecules (acetyl), and two one-carbon molecules producing an additional two

NADH molecules. Each two-carbon molecule then enters the citric acid cycle (Krebs's Cycle), joining with the two four-carbon molecules producing a six-carbon molecule (isocitrate). The isocitrate goes into a series of conversions producing a five carbon (α-ketoglutarate), a four carbon succinyl-CoA, succinate, fumarate, malate, and, finally, oxaloacetate. In the Krebs cycle, two ATP molecules, the reduction of six NADH molecules, and two $FADH_2$ molecules are produced for each glucose (See figure 1.1.1) [2].

The electron transport chain (ETC) is the last stage of aerobic respiration and is the only step that utilizes oxygen. The main goal of the electron transport chain is to produce ATP, which also produces water as a final biproduct, shown in the equation for cellular respiration. The electron transport chain involves the transfer of high energy electrons through four intermembrane protein complexes that act as electron donors and electron acceptors via chemical redux reactions. During the transfer of electrons from one complex to another, protons ($H^+$ ions) are pumped across the membrane.

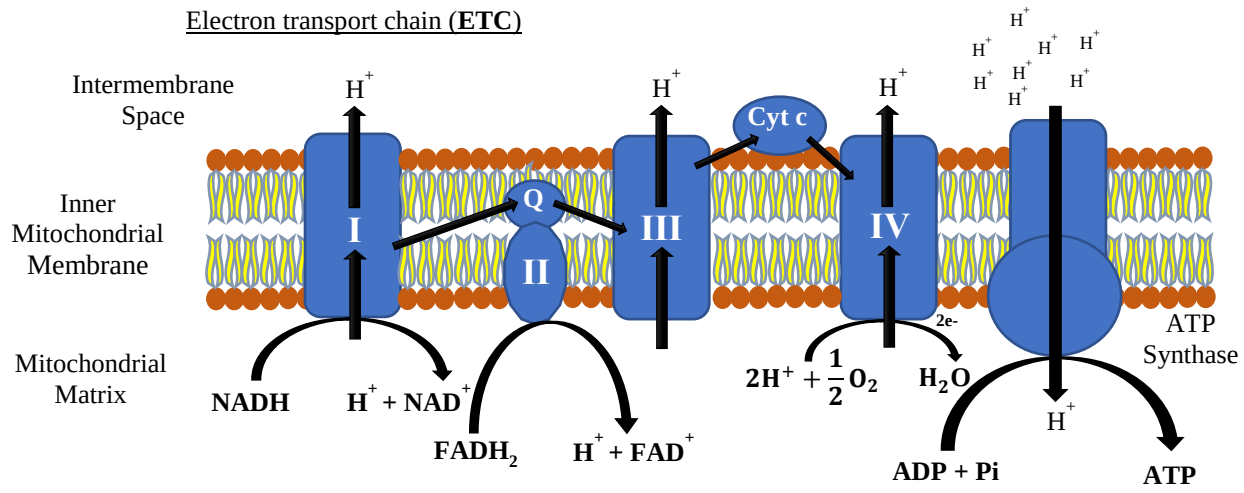


**Fig 1.1.2:** Electron transport chain explaining four complexes.

These electrons move quickly between each complex (See figure 1.1.2). In complex I, two electrons are accepted from NADH and four protons ($H^+$) are pumped across the membrane. Ubiquinol (UQ) transfers the electrons from NADH which oxidized to NAD. In complex II, two

electrons come across in the same pathway as $FADH_2$ which oxidized to $FAD^+$ moving an additional four protons ($H^+$) out of the mitochondria. Therefore, NADH and $FADH_2$ are known as electron carries. In complex III, an additional 2 protons are pumped out across the mitochondrial membrane. At the last complex, also known as complex IV or cytochrome c oxidase (CcOX) [2, 5], four electrons are transferred from cytochrome c to molecular oxygen producing water and pumping an additional 2 protons out of the mitochondrial matrix. In summary, a proton gradient is produced through the stepwise transfer of electrons from the high energy molecules NADH and $FADH_2$, with oxygen being the "terminal electron acceptor". This proton gradient produced from the ETC allows ATP synthase, an enzyme in the mitochondrial membrane to phosphorylate ADP to ATP. But, in *S. cerevisiae*, there is not the enzyme complex I in the yeast [5].

### 1.2 Role NADH in Metabolic Sensing

Autofluorescence is the naturally occurring fluorescence by biological structures which have been utilized to study biological processes [6]. Using the fluorescent properties of NADH, I am investigating the biophysical processes in cellular respiration to better understand mitochondrial function which will enhance our overall understanding of living cells and human health [3]. Because mitochondrial dysfunction is exceedingly related with many diseases such as cancer and Alzheimer's diseases etc, increasing our understanding of these mitochondrial processes could aid in developing cures and treatments [3]. Because yeast are single celled eukaryotic organisms, they are important models for human cellular function. 30% of human diseases depend on cellular functions that can be modeled by yeast activity. Thus to understand cellular function in metazoans we must understand more detail about the complex cellular processes and pathways of single celled eukaryotes [7].

The absorption spectrum of $NAD^+$ has a signal peak at 260 nm while the absorption spectrum of NADH has a peak at wavelengths of approximately 260 and 340 nm respectively. While excitation of the reduced and adenine nicotinamide ring (NADH\$NAD^+$) is absorbed at wavelength of maximum intensity of approximately 450 nm [8] (See figure 1.2.1).

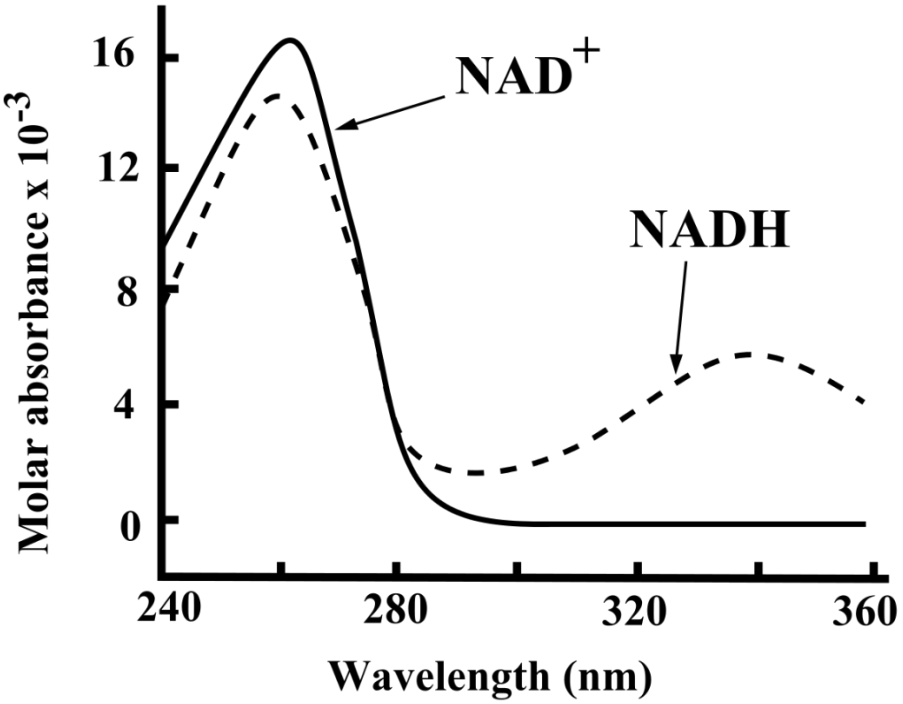


**Fig 1.2.1:** The absorption spectrum of NADH\NAD$^+$ [9].

To begin studying the role of NADH in metabolism, we need to understand the link between the autofluorescence spectrum shape and the metabolic activity during respiration. Investigation of the change in spectrum shape in response to a specific perturbation of metabolism will inform a biophysical interpretation of a change in spectrum shape. Utilizing the spectral differences in two known conformations of NADH, the free and protein-bound conformations, both of which have a different in peak emission wavelength and excited state lifetime, we can study the change in proportion of the two conformations [3]. Free NADH form is longer wavelength bound-protein NADH form. Average excited state lifetime of free is 0.4 ns but the protein bound NADH is 5 ns [10] (See figure 1.2.3).

The molecular structure of NADH consists of a nicotinamide ring and an adenine ring and can be found in an oxidized (NAD$^+$) form or a reduced (NADH) form [10] (see figure 1.2.2). Although NADH can take many conformations, we can characterize its conformation spectrally as being in either a folded or unfolded conformation, which can be distinguished by differences in the excited state emission spectrum. In cells, when NADH is bound to a membrane protein, it is in its unfolded conformation, and is in the folded conformation when it is free in the cellular

fluid. Spectral measurements can be used to analyze the cellular proportions of free and protein-bound NADH forms serving as a metabolic indicator and biomarker [11]. Knowing the difference in the proportion of the free and protein-bound conformations of NADH in the cell provides insight into the cells electron transport chain, while the protein-bound NADH represents the cell's energy reserve.

To monitor free and protein bound NADH conformations, we can use time-gated detection after pulsed excitation to obtain nanosecond-resolved emission spectra [12]. It allows for long excited-state lifetime autofluorescence to be monitored separately from the spectrum as a whole [11]. Utilizing the differences in excited state fluorescence lifetime, the proportion of free and protein bound NADH change according to cellular conditions [12]. By chemically inhibiting certain cellular processes, we can intentionally alter the proportion of each form. For example, the proportion of free and protein bound NADH after the addition of potassium cyanide (KCN), a complex IV inhibitor, and is an important indicator to investigate the cellular metabolism inside the cells.

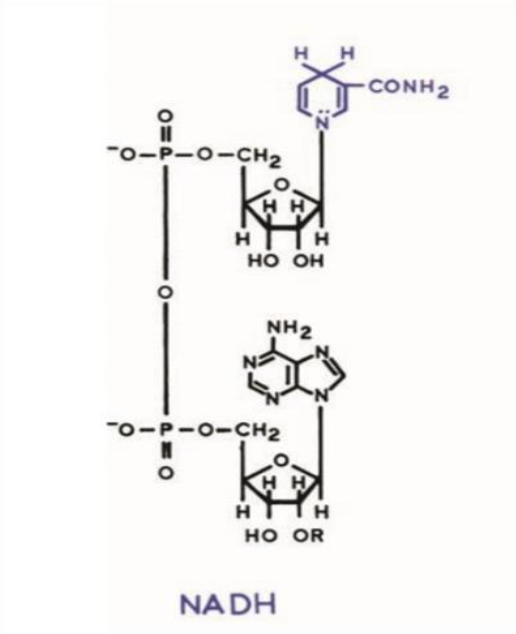


**Fig 1.2.2:** Top structure is the reduced nicotinamide ring and lower structure is the adenine nicotinamide ring [10].

### 1.3 Effect of Cyanide on Metabolism

Potassium cyanide (KCN) is a chemical compound known to take part in many chemical processes. Cyanide (CN) consists of a carbon atom triple-bonded to a nitrogen atom. Previously researchers have selected and studied cyanide for biological studies because it is one of the few water-soluble inhibitors able to cross the inner mitochondrial membrane [8]. Cyanide is known to inhibit the aerobic oxidative pathway. Once inside the mitochondrial matrix, cellular respiration is inhibited at complex IV changing the proportion of free and protein bound NADH and thus changing the autofluorescence signal [5, 12]. Previous researchers have investigated the sensitivity of three various functions of the cyanide action in complex IV, which are the effect of cyanide identifies oxygen consumption, mitochondrial membrane potential (proton transport), and the enzyme affinity to oxygen [5, 13, 14]. Although cyanide has three main effect on mitochondria function, we study them indirectly the effect on NADH Florence. The effect of cyanide is dependent on the cellular concentration, and at the organismal level the cardiovascular, respiratory, and central nervous system response is dependent on the quantity an individual may have consumed [13, 15]. Therefore, cyanide can play a significant role as a respiratory chain inhibitor dependent on its concentration and is a useful chemical to perturb a cell's metabolism.

Because cyanide has known effects on cellular metabolism, spectral shape changes from normal cellular respiration conditions to after the addition of cyanide allows biophysical interpretations to be drawn from the spectral shape change. To understand the concentration dependence of KCN on cellular respiration in the cells, we added cyanide at concentrations ranging between 1μM to 10mM. Applying a spectral phasor technique to investigate spectral shape change after the addition of cyanide allows for the cyanide response to be tested as two-state mode (More details is available in chapter 2 and 3). In this study the cellular metabolism of yeast is optically monitored using the autofluorescence signal of NADH from a solution of cells before and after the addition of a range of concentrations of cyanide.

Another part of my research is the addition of D-glucose. We have investigated about the effect of D-glucose on the response metabolism of cyanide added. The simplest of the D-Glucose molecular formula $C_6H_{12}O_6$ is also known as dextrose which occurs widely in nature. But, there is other kinds of sugar which are known L-glucose and 2-deoxy-D-Glucose. L-Glucose has a same molecular formula $C_6H_{12}O_6$, but it is a different structure and 2-deoxy-D-Glucose is a

different molecular formula $C_6H_{12}O_5$ which has 2-hydroxyl group replaced by hydrogen (See figure 1.3.1).

D-Glucose takes part in the first steps during cellular respiration in glycolysis when it is split into two which facilitates the reduction of NADH/ $NAD^+$. The pyruvate then can either take part in the Krebs's Cycle, which leads to the cell's main source of ATP, or can take the fermentation pyruvate pathway [5]. It determines ATP production in the cytosol of glycolysis and in the mitochondria by oxidative phosphorylation [5]. Higher concentrations of glucose stimulate the regeneration of NADH from $NAD^+$, which increases the overall production rate of ATP [16]. Thus, D-glucose added provides an increase in the amount of ATP in the cells [8,18].

Glucose plays the fundamental source of energy and carbon for cellular reparation and it plays a role in metabolic pathways [17]. Therefore, added D-glucose will increase rate of energy production which produces a change in metabolism that can be resolved spectrally. My experiment then focuses on the simultaneous additions of glucose and a wide range of concentrations of cyanide and to the sample to observe the different autofluorescence responses. Depending on the concentration of glucose available to the cell, the amount of NADH increases in cellular respiration in glycolysis, pyruvate, and Krebs's Cycle sequentially, thus causing totally different autofluorescence responses of free and bound NADH proportion after the addition of cyanide (KCN).

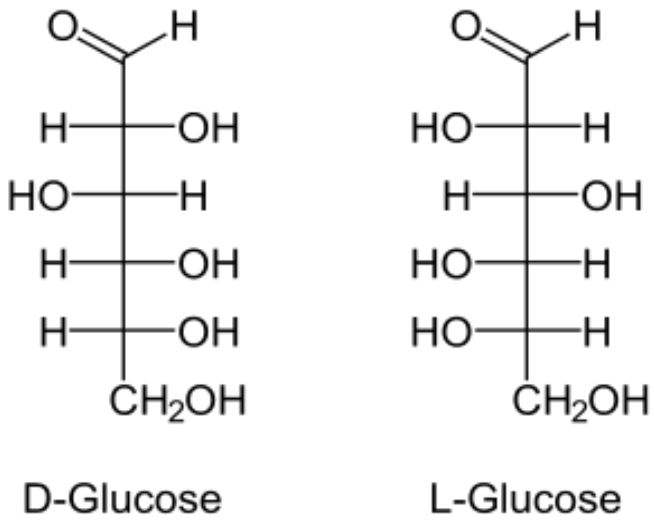


**Fig 1.3.1:** D-glucose on the left and L-glucose on the right [18].

### 1.4 Thesis Goals

The main approach of my thesis is to use the spectrum shape from the autofluorescence emission of light to describe the biophysical characteristics of mitochondrial function. Using our time-gated spectroscopy system, time-resolved information about the metabolic response to chemical perturbations can be obtained. Information will be gathered from the effects of cyanide and D-glucose on a cellular sample. From this purpose, combining all these of techniques are to get additional information being in more details an interpretation of the conformation changes between the free and protein-bound NADH forms during metabolism transition.

**I-** The first goal in this thesis is to examine the autofluorescence response at different concentrations of cyanide to better understand how NADH conformational changes during the metabolism transition. The goal is to extend upon the research of a previous graduate student (Madhu's). Like the previous research, I am using a wide range of concentrations of cyanide to study the concentration dependence of respiratory inhibition in protein complex IV in the mitochondrial membrane. Particularly, I aim to show how the different concentrations of cyanide effect on NADH conformational changes by using time gates and spectral phasor technique to get assessment of two state behavior.

**II-** The second goal is to extend the results of goal one by adding both D-glucose and cyanide to the sample to study the way glucose changes the effect of cyanide on mitochondrial function. To accomplish this, we study how the change in the proportion of the conformation of free and protein bound NADH by comparing the response for both measurements with glucose and non-glucose the changes the different in path directions and positions of spectral phasor. Another aim is to use the addition of D-glucose a test to know how it effects on cyanide as a respiratory chain inhibitor and a chemical to perturb the metabolism.

# Chapter 2: Material and Methods

This chapter explains steps for preparing the sample, preparing chemicals used, then explain techniques used to collect and analyze data.

## 2.1 Cellular Methods

### 2.1.1 Preparation of Cellular Samples According to Previous Section

Dry *Saccharomyces cerevisiae* yeast powder has been used in the preparation of the sample for this study. Roughly1 g of dry *S. cerevisiae* powder (Fleischmann's Active Dry) is mixed with 10ml of phosphate-buffered saline (PBS, cat. no. 20012, Life-Technologies) and then is left in the PBS to be activated [5]. To be sure the tools of the lab are clean, we use the gloves and ethanol. Next step, the sample of cellular suspension is stirred and covered with Parafilm to prevent any air passing through it. Then, a micro-spatula is soaked into the suspension and streaked to an YPD (yeast extract peptone dextrose) agar plate. Also, the plate converts and inverters to prevent any air impurities entering and any glue culture. YPD agar plate is kept upside down to avoid condensation from falling into the growing culture. After leaving that plate in this position for 2-3 days, the first of the yeast plate is ready to harvest. We do not need to grow the yeast from powder every time. Instead, we can transfer the culture to new plates every 5-7 days. Also, the lab is not temperature regulated room temperature was measured at $22 \pm 2$ ℃ [19].

In order to prepare suspension, a loop full of yeast is mixed with 1000µl of PBS and then placed into a centrifuge lightly then the liquid is removed. This is repeated three times to remove fluorescence background coming the growth medium. Finally, the sample is done after adding 2000µl of PBS to the 1cm-quartz cuvette for a final volume of 3000µl. A magnetic stir bar is placed inside the cuvette and the sample is left in open air for around 20 minutes letting cells to be more acclimated to a new medium. The sample is then ready to take measurement for my experiment.

### 2.1.2 Preparation of Cyanide and Glucose Solution

Potassium cyanide is a compound with the formula KCN. Potassium cyanide powder is used to prepare of the stock solution approximately 500mM in 50ml volume in the PBS. We have used around 1.628g of KCN powder to put in the PBS at room temperature. In my

experiment, we have used the range concentrations from 1µM to 10mM. The final concentrations of cyanide used are 50µM, 100µM, 250µM, 500µM, 700µM, 900µM, 1mM and 10mM.

In order to not change the emission intensity significantly due to a dilution in cellular concentration, when the cyanide solution is used to induce a cellular response, not more than we do without increase volume more than 2% therefore a fifty time more concentration stock solution is used. For example, I have used 5000µM to produce a final concentration of KCN of 100µM (See table 2.1.2.1).

**Table 2.1.2.1:** The concentrations and volumes of cyanide used in this experiment.

| Final Concentration of KCN | Stock Concentration of KCN | The Volume of KCN Added to 3ml of Sample |
|---|---|---|
| 100µM | 5000µM | 60µl |
| 250µM | 12500µM | 60µl |
| 500µM | 25000µM | 60µl |
| 700µM | 35000µM | 60µl |
| 900µM | 45000µM | 60µl |
| 1mM | 50mM | 60µl |
| 10mM | 500mM | 60µl |

Another chemical added is the sugar D-glucose. It plays the fundamental role in many cellular processes like reduction and oxidization of NADH/$NAD^+$ and the production of ATP. Thus, we want to know how the change in the proportions of free and protein bound NADH change according to cellular conditions when both D-glucose and cyanide are added. I have produced 600mM in 10ml volume as stock solution by using 1.0809 gram of D-glucose in 10ml volume in PBS. We are added 15µl D-glucose to the sample after 15 minutes to get 3mM the final of D-glucose concentration. Then, the same experimental procedures are carried out, measuring the cyanide response after D-glucose is added. The cyanide response is monitored with D-glucose and without D-glucose.

## 2.2 Optical Methods

### 2.2.1 Measurement Optical Density

Optical density (OD) or absorbance of the sample is measured before starting the metabolic monitoring measurement. Optical density of the sample should be from 1.0 to 1.3 so that the cell concentration has a linear relation with the emission intensity. At this range of OD, the cellular suspension has a density of approximately $10^7$ cells/ml as measured by hemocytometer (See figure 2.2.1.1). We report the optical density at wavelength 600 nm. The optical density is computed by,

$$OD_\lambda = Log_{10}\left[\frac{I_o}{I}\right] \qquad (2.2.1.1)$$

Where $I_o$ is the lamp intensity of wavelength $\lambda$ after passing through the reference sample (PBS), and I is the lamp intensity at wavelength $\lambda$ after passing the sample.

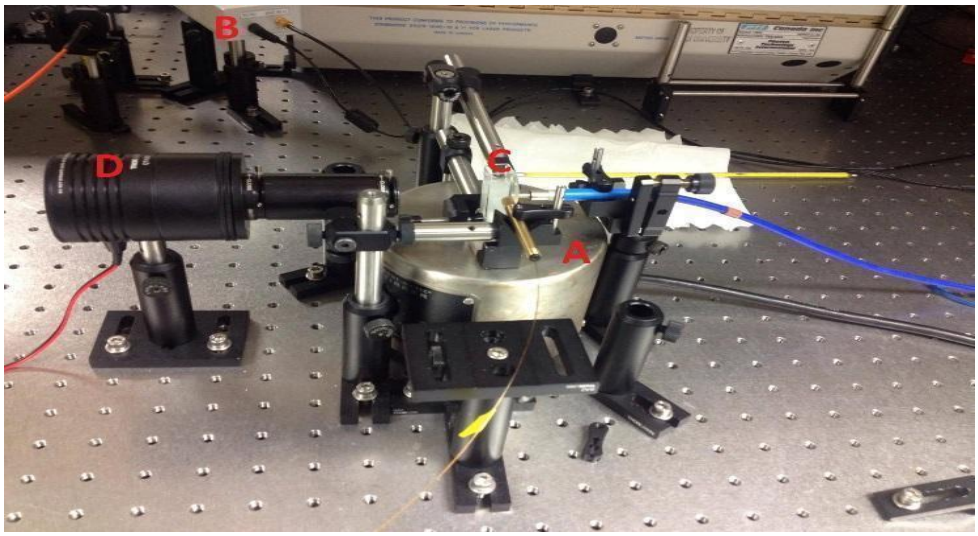


**Fig 2.2.1.1:** Cellular measurement setup. A (magnetic stirrer), B (optical discriminator), C (sample), D (lamp used for measuring OD).

### 2.2.2 Experimental Step

The experimental technique used is fluorescence spectroscopy. Our system consists of a nitrogen laser (Model Gl-3300, Photon Technology International, PTI, Canada), optical fiber, spectrograph (model MS 125, Spectra-Physics/Newport), and ICCD (Intensified Charge Coupled Device). The ICCD utilizes a 1024 x 1024-pixel chip, fully binned along one axis during readout, resulting in a 1024-spectral-channel output, and sample stage. The optical discriminator is used so that it sends out the pulse to ICCD when it detects the laser. The emission from the sample is sent to ICCD with the help of another optical fiber at 90 degrees to the excitation fiber to block any transmitted light from reaching the emission fiber. The fluorescence emission is used filtered 385mm-long pass filter because it prevents UV radiation from the sample. Quartz cuvettes are used for data measurements to avoid any fluorescence coming from the plastic. The sample is kept at uniform concentration using a magnetic stir-bar to keep the cellular sample from settling during the measurement [11] (See figure 2.2.2.1, and 2.2.2.2).

A 1μM solution of rhodamine B in ethanol solvent is in a cuvette the place of sample fluorophore to confirm the optimize alignment. We got approximately 800 detect account in the pulse laser without gain. The sample is excited by a nitrogen laser with a 1ns nominal pulse width at a repetition rate of 3 Hz with an emission wavelength of 337nm. The pulse coming out of the nitrogen laser then passes through a 25-m optical fiber to delay the excitation pulse from arriving at the sample before the ICCD is ready to collect emission signal because there is a minimum time between detector triggering and intensifier gate opening (additional details are found in this paper) [12].

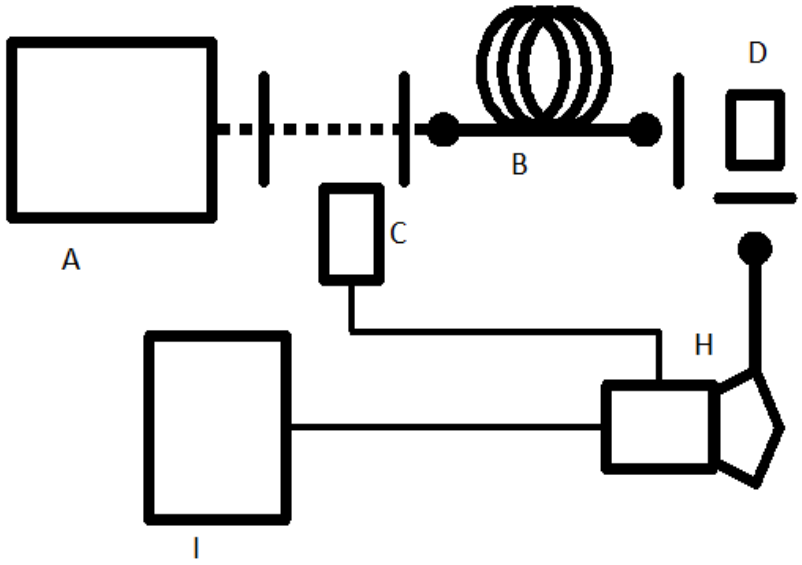


**Fig 2.2.2.1:** Schematic representation of the time gated system. Dotted lines are used to show optical pathways while solid lines are used to show the electronic pathways. A (nitrogen laser), B (optical delay fiber), C (optical discriminator), D (sample), H (ICCD and spectrograph coupled), I (control computer) [12].

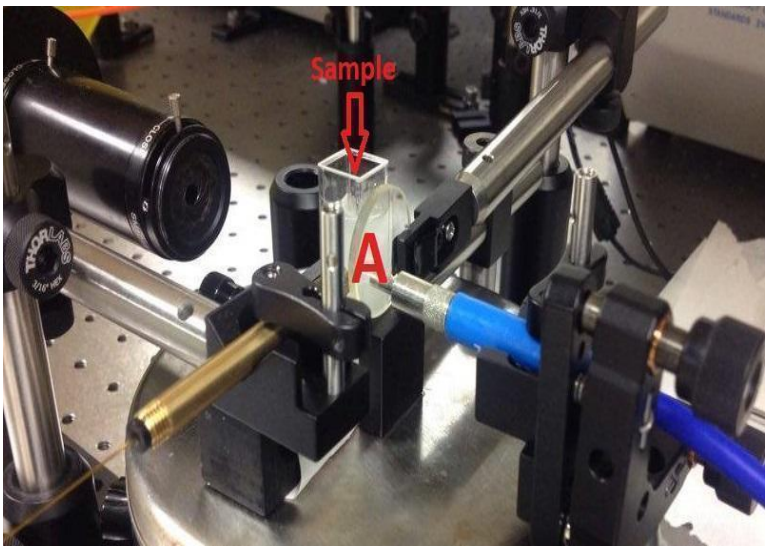


**Fig 2.2.2.2:** Apparatus setup during the cellular measurement. Cell sample being excited with the laser coming through brass fiber and fluorescence emission passing through blue fiber. A (long pass filter).

For our metabolic measurements two-time gating schemes are used. The full gate collects the entire emission spectrum, which has condition that is a time integrated autofluoresence signal. The late gate samples the emission spectrum at a delayed time, corresponding to the long excited-state lifetime emission and has condition that is time-gated autofluorescence signal. Spectra are taken every 15-30 seconds.

ICCD gate width around 80 ns was used to reject ambient light during spectral acquisition, and a full spectrum was collected for each excitation pulse although spectra were averaged over multiple pulses for a peak-signal-to noise ratio (SNR) [11]. The time delay ($t_{delay}$) signifies the spectral acquisition delay time determined from a reference time generated by a constant fraction optical discriminator sensing the laser pulse. late gate is the timing parameter, which is varied from trial to trial to observe different portions of the autofluorescence signal, while it start to collect after peak intensity around 3ns and it constants at 5ns [12] (See figure 2.2.2.3). The time width ($\Delta t_{gate}$) the time window, or the amount of time that the autfluorescence acquisition is taken.

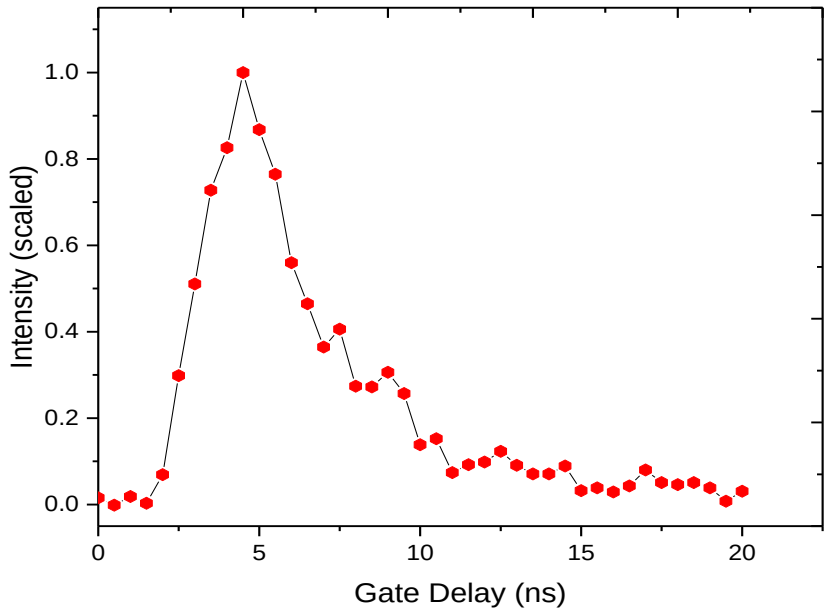


**Fig 2.2.2.3:** Time-gated autofluorescence intensity to show the gate delay $t_{delay}$ at a gate width $\Delta t_{gate}$ =5ns.

Time gated fluorescence spectroscopy is a utility to measure the amplitude of chemical measurements without damaging the cells providing real-time structural and dynamic information which can be used to study biophysical systems. Thus time gated spectroscopy is an invaluable technique in chemistry, physics, and biomedical sciences for aiding in both qualitative and quantitative analyses [6] (See figure 2.2.2.3). The quantitation of autofluorescence spectrum can show the small spectral emission peaks (~15 nm) observed between free and protein-bound NADH forms [11].

To study the change in proportions of free and bound NADH, we utilize both autofluorescence signals from the full gate and the late gate. The full and late gate signals are used to distinguish between the free and bound NADH forms based on their difference in average lifetime. The late gate signal tells us about the long lifetime protein-bound NADH forms while the full gate signal tells us about the whole signal. The full gate collects data by acquiring the entire autofluorescence signal, and the late gate collects data using a delayed autoflourescence acquisition. This information is very important to study the cells metabolism as it provides a ratio between the two forms of NADH. During the experiment, we monitor the intensity vs. time, and add KCN when a steady baseline is established. In both the full and late gate, the intensity goes up when we added the different concentrations of cyanide to the sample because of an increase in cellular NADH concentration.

### 2.2.3 Spectral Phasor Analysis

The spectral phasor analysis is a sensitive technique that can be used to detect small changes in spectrum shapes and can be used to test for two states behavior. Spectral phasor analysis generates an easily interpreted graphical representation of spectral changes. We are utilized a spectral phasor technique which produces a two-dimensional plot using the real and imaginary components of the first harmonic of the spectrum's Fourier transform [20]. A spectral phasor plot is beneficial because data points calculated from spectra of similar shape tend to cluster and that phasor points coming from two-component system lay along a line [21]. It can distinguish different metabolic states through label free FLIM. The spectral phasor analysis technique has technologically advanced with Fereidouni et al., [20, 22, 23]

For $N$ spectral channels, the phasor $A$ is:

$$A = \sum_j F_j \; e^{i\frac{2\pi}{N}j} \qquad (2.2.3.1)$$

Where the sum is done over spectral channel *j* (i.e. detector pixel) and $F_j$ is the intensity for chemical *j*, normalized to the integrated intensity. The real and imaginary components of spectral phasors are given by:

$$Re(A) = \sum_j F_j \cos\left(\frac{2\pi}{N}j\right) \qquad (2.2.3.2)$$

$$Im(A) = \sum_j F_j \sin\left(\frac{2\pi}{N}j\right) \qquad (2.2.3.3)$$

To confirm that spectral phasors from a two-component system lay along a line. We have been assuming that the measurement spectrum *F* to be linear combination of $F_1$ and $F_2$ and fraction *a*, which range starts from 0 to 1. Then, the spectral phasor changes:

$$A = \sum_j F_j \; e^{i\frac{2\pi}{N}j} \qquad (2.2.3.4)$$

$$A = \sum_j [aF_{1,j} \; + (1-a)\, F_{2,j}\,]\, e^{i\frac{2\pi}{N}j}$$

$$A = [\, aA_1 \; + \; (1-a)A_2\,] \qquad (2.2.3.5)$$

$$a = \frac{A - A_2}{A_1 - A_2} \qquad (2.2.3.5)$$

Therefore, for two component systems, phasor *A* lies a fraction along a line joining $A_1$ and $A_2$. The plot *Re (A)* and *Im (A)* when phasors lay along a line.

$$Im(A) = \left(\frac{(Im(A_1) - Im(A_2))}{Re(A_1) - Re(A_2)}\right) Re(A) + \frac{Re(A_1)\, Im(A_2) - Im(A_1)\, Re(A_2)}{Re(A_1) - Re(A_2)} \quad (2.2.3.5)$$

The fraction *a* is sensitive to spectrum shape, not intensity and it is calculated using spectra normalized to the integrated intensity. If the aim is to find the relative concentration, difference in quantum yield and the absorption cross section of the two components must also considered. To account for this, we define an empirical brightness *B*, such that

$$a \propto B_1 f_1$$

$$1 - a \propto B_2 f_2 \qquad (2.2.3.6)$$

Where $f$ is a fractional concentration. Thus,

$$\frac{a}{1-a} = \frac{B_1 f_1}{B_2 f_2} = \frac{B_2 f_2}{B_2 (1 - f_1)} \qquad (2.2.3.7)$$

Where $f_1 + f_2 = 1$. Solving for $f_1$ and $f_2$,

$$f_1 = \frac{a\frac{B_2}{B_1}}{1 - a + a\frac{B_2}{B_1}} \qquad (2.2.3.8)$$

$$f_2 = \frac{1-a}{1 - a + a\frac{B_2}{B_1}} \qquad (2.2.3.9)$$

Where $\frac{B_2}{B_1}$ is the of fluorophore brightness, found empirically under fixed measurement conditions by determining the emission intensity for samples serving at the *a*=0 and 1 references.

Once more, spectral phasor technique plays an essential role in the exploration of my analysis due to its ability to describe the relationship between two similarly shaped spectra. Spectral phasor analysis gives us a sense for how spectrum shape as represented on a phasor plot.

Spectral phasors are calculated from Gaussian-shaped spectra modifying wavelength and width from a crescent-shaped grid. Designed for Gaussian-shaped spectra modifying wavelength of fixed width from circular trajectories. The width of the spectrum increases, the spectral points gradually move from zero to infinity (to center). While, the spectral points move from the center to the left of a crescent-shaped grid when a spectrum width decrease. Due to being determined by values of the cosine and sine functions, the plot of spectral phasor components is calculated from Gaussian-shaped a unit circle in the delta function limit. (See figure 2.2.3.1) blue lines of connecting points of constant maximum wavelength, and red lines of connecting points of constant maximum width. Phasor plot trajectories of constant maximum wavelength and of constant width are almost orthogonal, therefore the most changes of discrimination in maximum wavelength and width are only negative real axis because the limit of increase of maximum wavelength and width have been centering in the wavelength interval for calculation this phasor.

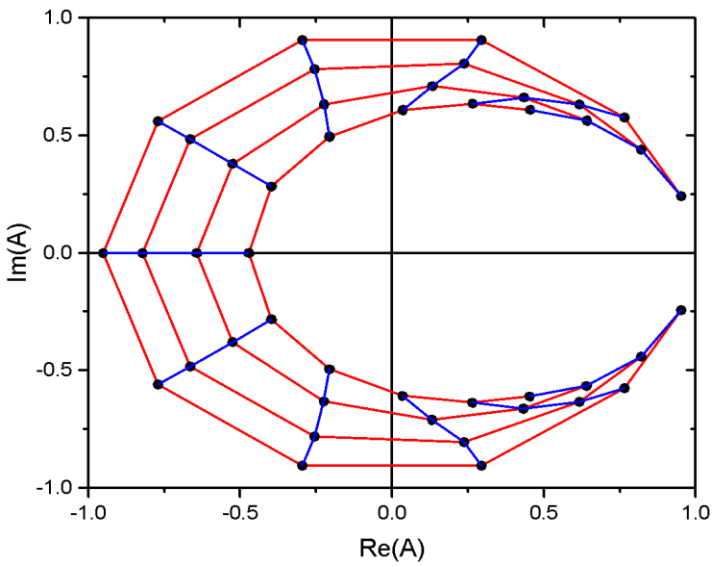


**Fig 2.2.3.1:** A plot of spectral phasor components calculated from Gaussian shaped spectra.

Phasor components are most sensitive to the behavior of the spectrum at wavelengths where the cosine or sine function change most rapidly (i.e., has the greatest first-derivative

magnitude). If the spectrum is centered in the wavelength interval, Re (A) part of the spectral phasor is sensitive to the spectrum width and Im (A) is sensitive to the spectrum's maximum wavelength.

A fundamental property of spectral phasor analysis is that a two-component system will lay along a line. An example of this is shown with mixtures the two fluorophores 9-anthracenecarboxylic acid (9CA) and 1.4-bis (5-pheny1-2-oxazolyl) benzene (POPOP) mixed at different ratios (See table 2.2.3.1). Data shown was obtained by Madhu Gaire, a previous graduate student in our lab, who used the fluorophores 5μM (9CA) and 5μM (POPOP) in a different ratio (See figure 2.2.3.2) [23].From the plot, the spectral phasor points are all obviously along a line connecting the pure fluorophore samples, they are collinear indicating a two-component state.

**Table 2.2.3.1:** measurement of mixture of POPOP and 9CA.

| POPOP (ml) | 9CA (ml) | Final volume (ml) |
|---|---|---|
| 3 | 0 | 3 |
| 2 | 1 | 3 |
| 1.5 | 1.5 | 3 |
| 1 | 2 | 3 |
| 0.9 | 2.1 | 3 |
| 0.8 | 2.2 | 3 |
| 0.7 | 2.3 | 3 |
| 0.5 | 2.5 | 3 |
| 0.3 | 2.7 | 3 |
| 0.1 | 2.9 | 3 |
| 0 | 3 | 3 |

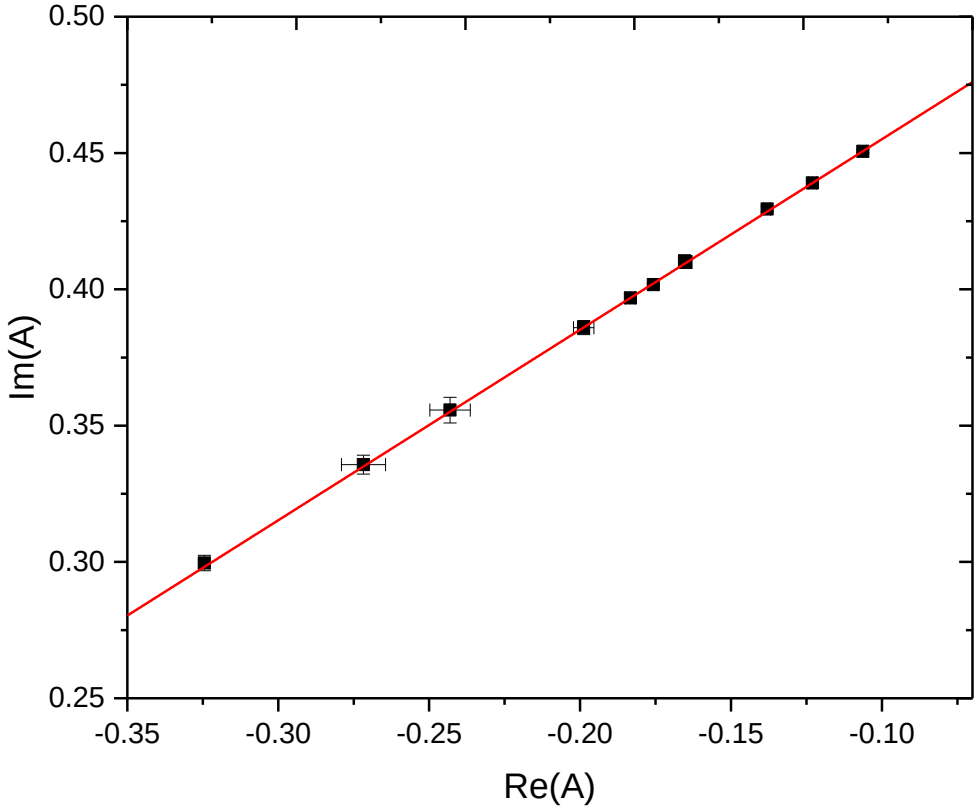


**Fig 2.2.3.2:** Spectral phasor plot pf POPOP and 9CA mixture.

## Chapter 3: Result and Discussion of Glucose vs. no Glucose Responses

This chapter is divided into three sections. First, we discuss the autofluorescence intensity vs. time, the spectral phasor analysis and the discussion. The second section discusses these same steps with the addition of D-glucose because it can be used as a test to know how it effects on cyanide as a respiratory chain inhibitor and a chemical to perturb the metabolism. Finally, we focus on additional discussion.

### 3.1 Autofluorescence Response with Various Concentrations of Cyanide (no-Glucose):

#### 3.1.1 Autofluorescence Intensity vs. Time

My work is focused on different responses that cyanide can make, by changing the concentrations added. The final cyanide concentrations are 10mM, 1mM, 900μM, 700μM, 500μM, 250μM, 100μM, and 50μM in the volume 3ml. For each experiment, cyanide is added from the fifty times more concentrated stock solution. In each concentration, we monitor the intensity vs. time as detected using full gate and late gate measurement. Full gate measures the free and protein-bound NADH and the late gate measures protein-bound NADH only. The time axis is shifted, so that, the time is zero when the cyanide is added (See figure 3.1.1.1). In all cases, we notice that the intensity increases when the cyanide is added. The larger intensity increase is seen with the highest cyanide concentration, and the intensity change becomes smaller as the concentration of cyanide decreases (See figure 3.1.2.1). Likewise, in all the plots the fraction of full gate (blue) intensity vs. time are increased more than late gate measurements (red). Additionally, we did four independent measurements for each cyanide concentration with no-glucose (See Appendix for all data sets).

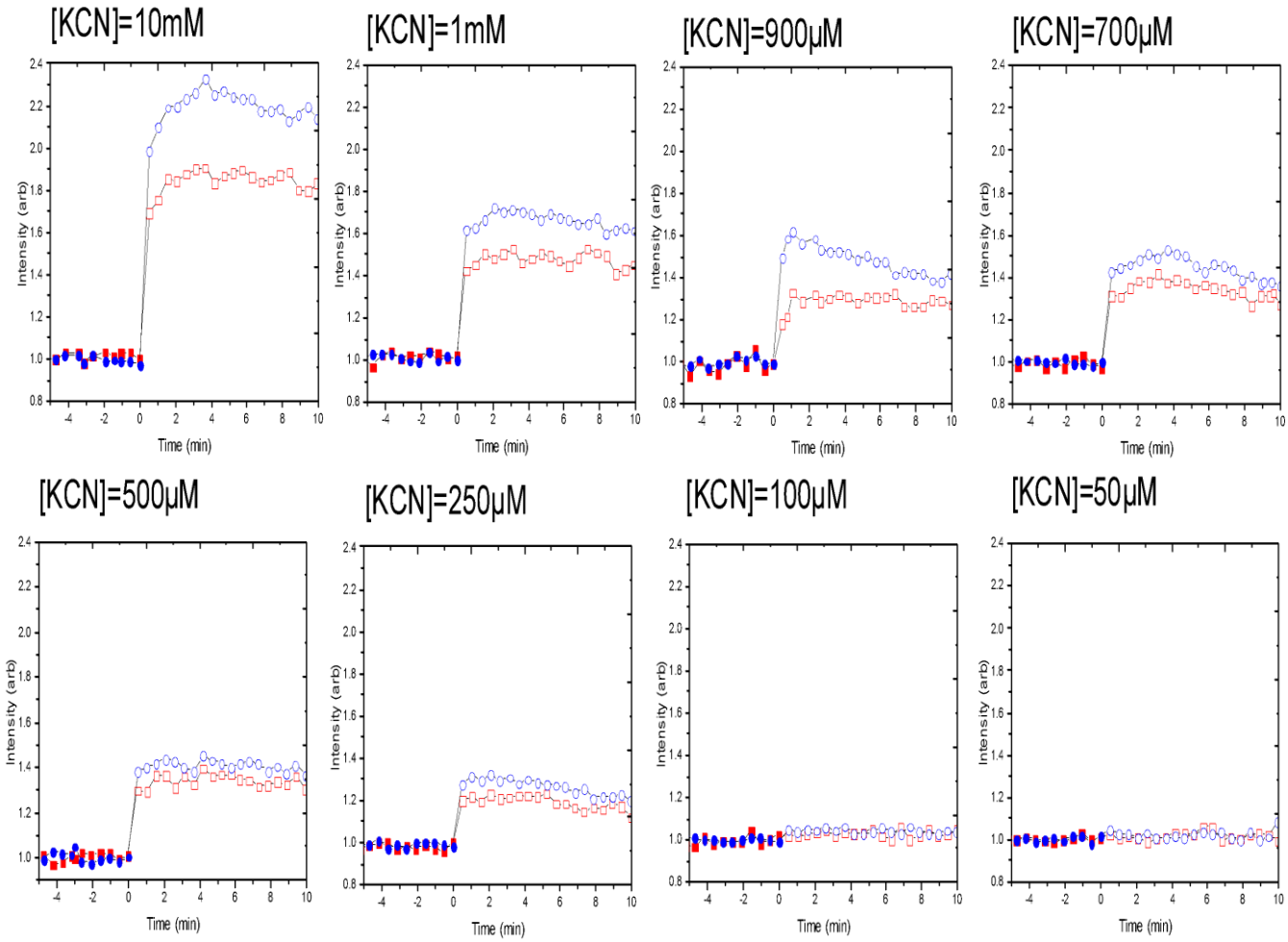


**Fig 3.1.1.1:** Monitoring autofluorescence response to cyanide additions. In all figures, full gate data are blue circles, and late-gate data are red squares. Each data point is a spectrally integrated intensity versus time, normalized to the intensity prior to chemical addition (Cyanide). Filled symbols are before cyanide addition and open symbols are after cyanide addition. Similarly, figures are shown on the (top) for addition of 10mM, 1mM, 900µM and 700µM cyanide. On the bottom, 500µM, 250µM, 100µM, and 50µM of cyanide.

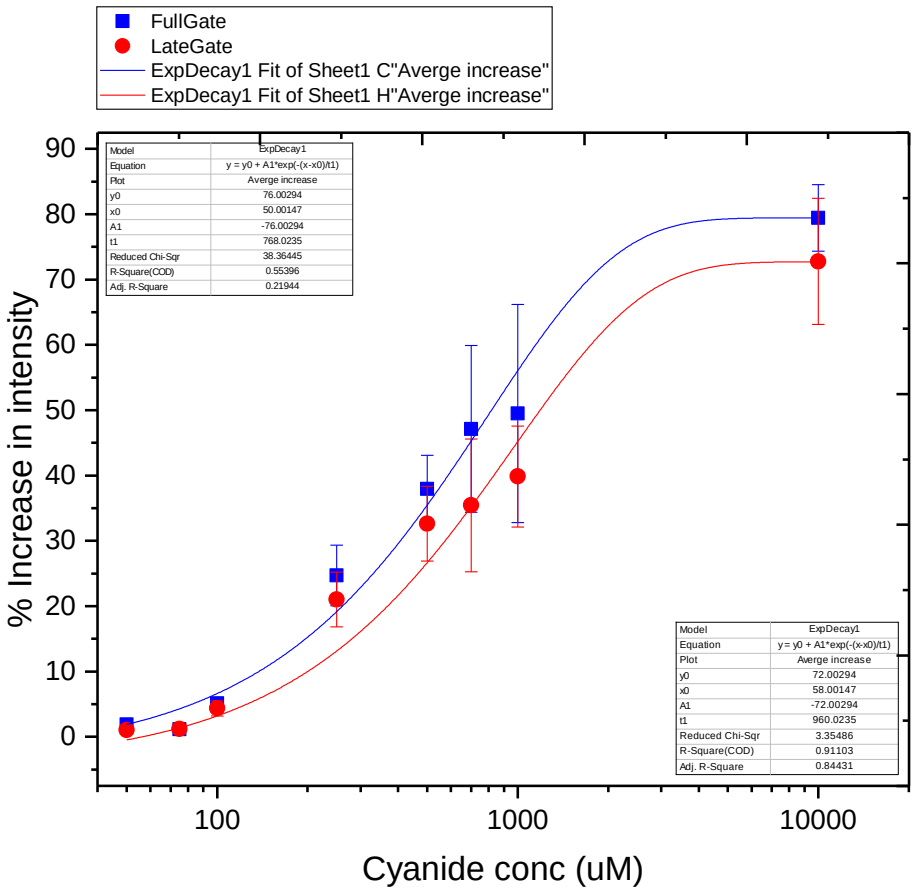


**Fig 3.1.1.2:** Percentage in intensity vs concentration of cyanide. Red filled circles are shown late gate data and the blue filled squares are shown full gate data.

Previously, Madhu has found that there is an exponential increase in intensity with increasing cyanide concentrations for the full gate measurements only [23]. However, we go beyond his study by having both full and late gate measurements. We have observed the intensity increase fits an exponential curve with increased concentrations (See figure 3.1.1.2). It is highly interesting due to the late gate data showing a different percentage increase than the full gate response. In low concentrations almost show us the same percentage between two gates in 50µM, 100µM, 250µM. We have seen that as an empirical fit, almost our data points fit well and consistent to an exponential function. But, the error bar for 1000µM is larger than other because the percentage increase in intensity is much greater than the smaller sample concentrations, thus it is expected to have larger intensity variation. Now, we use the spectral phasor analysis to

interpret whether the response in the low concentration regimes differs with those in the high concentration regimes.

### 3.1.2 Discussion of Intensity vs. Time

Through the work in my experiment, when we have used many concentrations of cyanide as a starting from 10mM to 50μM, it shows that cyanide binds the oxidized form of NADH/$NAD^+$, inhibiting proton transport ($H^+$), and reducing enzyme affinity to oxygen in the complex IV in the electron transfer chain (See figure 3.1.1.1). The intensity goes up when we add the different concentrations of cyanide because KCN inhibits complex IV from cellular oxygen used and ATP production [4]. We observe the increase in intensity of each concentration of the cyanide added, because the concentration of NADH inside mitochondria is increased due to cyanide binding complex IV in electron transport chain and keeping it from being reduced. For example, the concentration of cyanide 10mM has 54.73 %, and 1mM has 39.68 % percentage etc. (See figure 3.1.1.2). The inhibiting action of cyanide is important because NADH is used as a metabolic indicator and biomarker and because the various NADH forms respond directly to changes in mitochondrial function. We utilize the monitoring technique to investigate the autofluorescence response of cellular suspensions to additions of cyanide, an inhibitor of cellular respiration.

Due to a different percentage intensity increase, which is depending on the concentration of cyanide added, we can track the cell's metabolism as a function of cyanide concentration. After analyzing the data, we further have seen that measurements of full gate have more amounts than the late gate as expected because the full gate shows the time integrated autofluorescence while late gate shows the time-gated autofluorescence signal. Therefore, cyanide plays a significant role as a respiratory chain inhibitor dependent on its concentration and is a useful chemical to perturb a cell's metabolism.

Again, the late gate signals tell us about the long lifetime protein-bound NADH forms while the full gate signals tell us about the whole signal. Or, the full gate collects data by acquiring the entire autofluorescence signal, and the late gate collects data using a delayed autoflourescence acquisition. I think the reason to look to full gate and late gate data because we observe the full gate has some percentage and late gate has a different percentage, so time gate has different percentages in all concentrations of cyanide. Therefore, this data gives us more

details about dynamics where the dynamic of rise in concentration for protein-bound NADH form is a different response. In cells, when NADH is bound to a membrane protein, it is in its unfolded conformation, and is in the folded conformation when it is free in the cellular fluid (See figure 3.1.1.1). We get information by distinguishing the differences in the excited state emission spectrum where the free and protein-bound NADH do not track perfectly with each other by monitoring cyanide response with time. After a few minutes we can observe the level of conformations of dynamic in both gates decrease because the complex I, and II are still working in same quality so, they often consume some values of NADH in mitochondria of cells for example, 250µM, 700µM, and 900µM (See figure 3.1.2.1). Therefore, this information is very important to study the cells metabolism as it provides a ratio between the two forms of NADH.

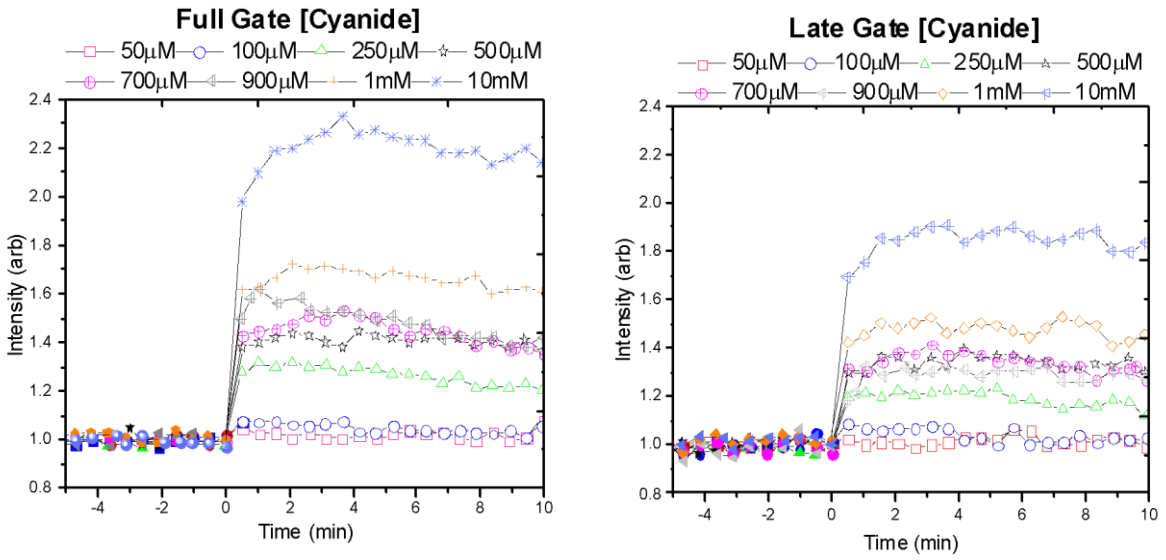


**Fig 3.1.2.1:** Monitoring autofluorescence response to cyanide additions. In the figure, full gate data, spectrally integrated intensity versus time, and late gate data, spectrally time-gated autofluorescence, normalized to the intensity prior to chemical addition (cyanide). Autofluorescence spectra filled symbol (before cyanide addition) and open symbol (after cyanide addition). Similarly, figures are shown on the (left) full gate data and, on the (Right), late gate data for addition of 10mM, 1mM, 900µM, 700µM, 500µM, 250µM, 100µM and 50µM of cyanide.

### 3.1.3 Spectral Phasor Analysis

For every intensity measurement there is a full spectrum available, and using those spectra we have calculated the spectra phasor points to see how the phasor change when we add cyanide by using the equations as described in the previous chapter. We made the spectral phasor plot to show at high cyanide concentrations clear shifts are observed for the full (blue) and late gate (red). Moreover, for the cyanide concentrations that are lower we continue to observe that full and late gate shifts are not in the same direction. For example, the highest concentrations of KCN show greater shift in the imaginary axis until the lowest concentrations start to see the change shift behavior. In general, the full and late gate shift decreases, becomes more negative in both the real and imaginary directions with full gate shifts more so in the imaginary, and they will continue until at low concentrations shift the direction. Specially, the data points in experiments of low concentrations 50µM, and 10µM have been observed in different directions, but the data points in cases of 250µM, and 500µM and the higher concentrations of 1mM and 10mM have been observed in similar directions through cluster whereas the phasor points coming from two-component system lay along a line (See figure 3.1.3.1). And, we did four measurements on independent sample for each cyanide concentration with no-glucose (See Appendix for all data sets).

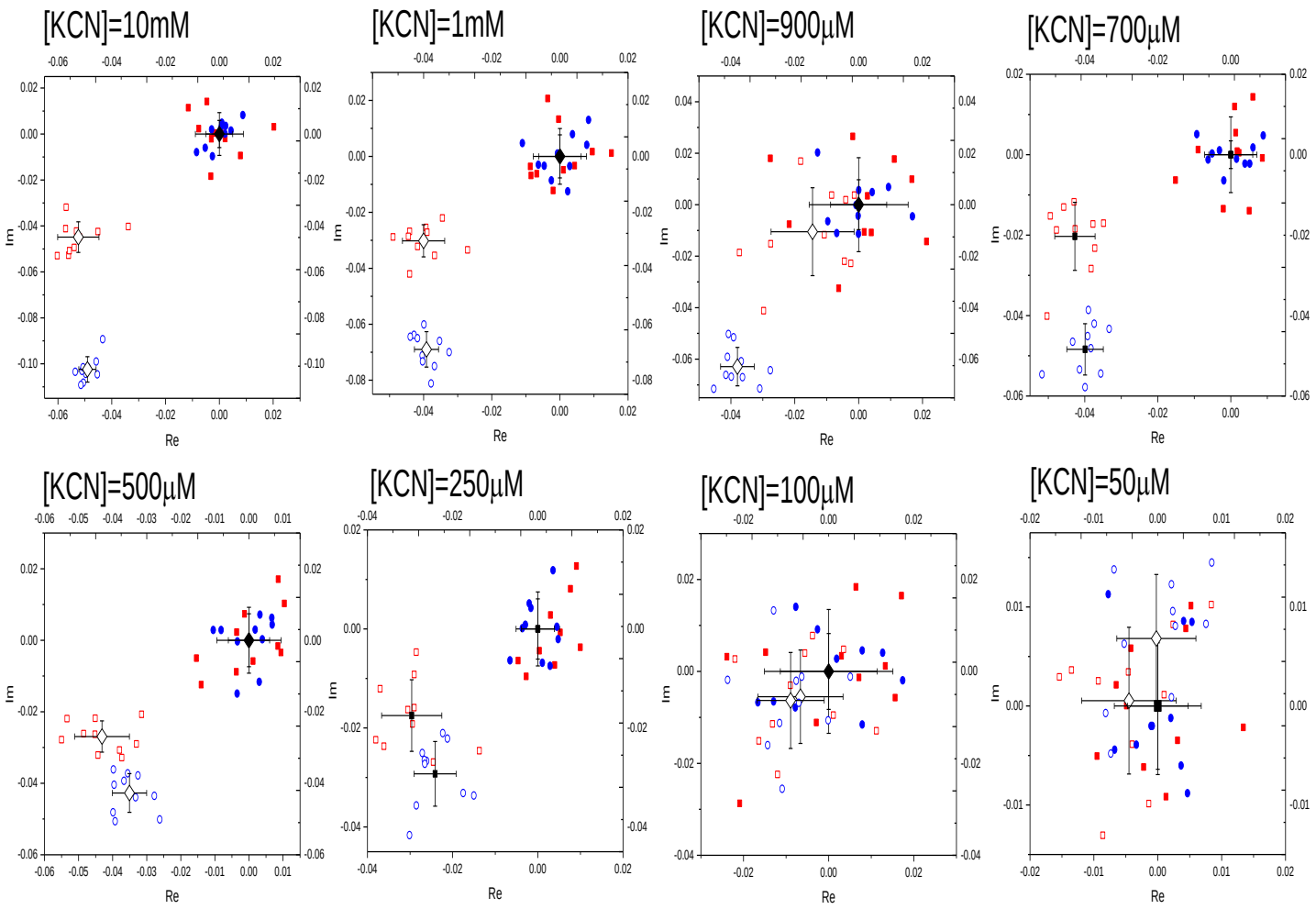


**Fig 3.1.3.1:** Spectral phasor plots for different concentration of cyanide added. In all figures, full gate data are blue circles, and late-gate data are red squares. Each data point is a spectrally integrated intensity versus time, normalized to the intensity prior to chemical addition (Cyanide). Filled symbols are before cyanide addition and open symbols are after cyanide addition. Similarly, figures are shown on the (top) for addition of 10mM, 1mM, 900µM and 700µM cyanide. On the bottom, 500µM, 250µM, 100µM, and 50µM of cyanide.

### 3.1.4 Discussion of Spectral Phasor Analysis

Using the spectral phasor analysis technique, we can assess whether observed spectral changes are consistent with a two-state model. In each experiment, we monitor the spectral phasor plot as detected full and late measurement. The imaginary and real axis shifted, so that, the both full and late gates is zero before the cyanide added (See figure 3.1.3.1). In general, the full gate decreases and shifts more negative in the imaginary and in the real direction more than in the late gate. Otherwise, these responses of full and late gate change direction at the low concentrations such as 50μM and 10μM. The observed phaser shift is dependent on the many different proportions of NADH conformations (the concentration of cyanide added), hence a change in spectrum shape coming from the change in proportion of NADH results in a spectral phasor plot shift. A point that is very important to help us understand the metabolic activity during respiration inside the cells is that the shifts of positions in spectral phasor technique depends on the changes in the peak position or/and width of spectrum shape after cyanide added.

Also, using the collinearity scheme, we observe that the spectral points of each of the lower concentrations are collinear in full and late gate, but in the higher concentrations, like with the 10mM, are non-collinear in both gates. Generally, we see that by this evidence for the spectral detection of a concentration-dependent cyanide action (See figure 3.1.4.1), the high concentrations of cyanide have a different shift in direction than in the low concentrations. This points to a concentration dependent mechanism of action of cyanide on cellular metabolism.

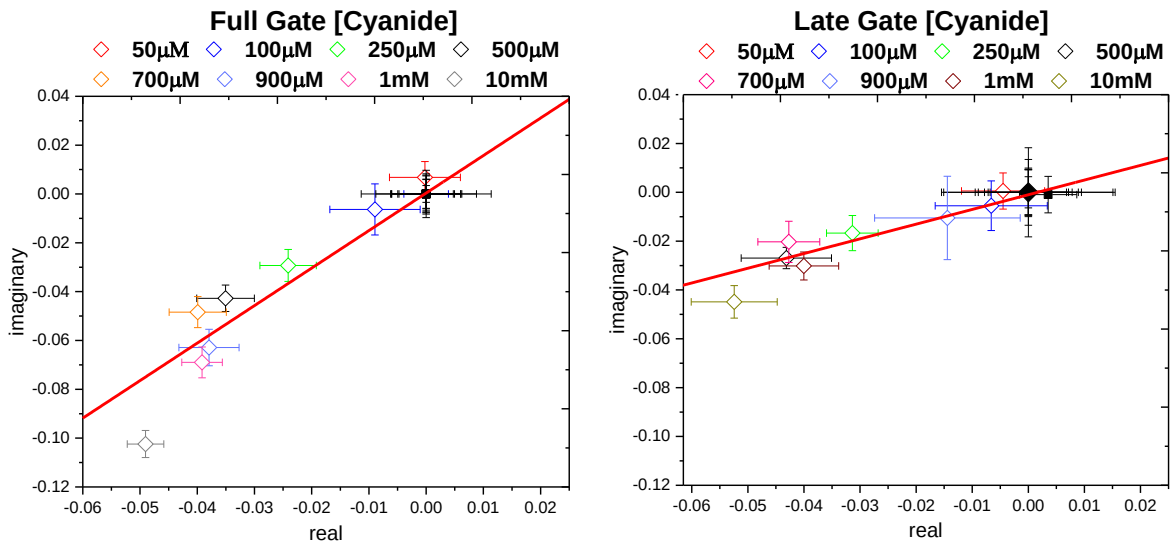


**Fig 3.1.4.1:** Monitoring autofluorescence response to cyanide additions. In the figure, full gate data, spectrally integrated intensity versus time, and late gate data, spectrally time-gated autofluorescence, normalized to the intensity prior to chemical addition (Cyanide). Autofluorescence spectra filled symbol (before cyanide addition) and open symbol (after cyanide addition). Similarly, figures are shown on the (left) full gate data and on the (Right), late gate data for addition of 10mM, 1mM, 900µM, 700µM, 500µM, 250µM, 100µM and 50µM of cyanide.

To verify that the plot of spectral phasor components calculated from Gaussian shaped spectra, which is coming from two components lie along a line, before and after addition of concentration cyanide. Gaussian shaped says that if the spectral points move from the center to the right of a crescent-shaped grid when a spectrum width increase (See figure 2.2.3.1), thus it applies on the concentration of cyanide 50µM, 700µM and 10mM (See figure 3.1.4.2).

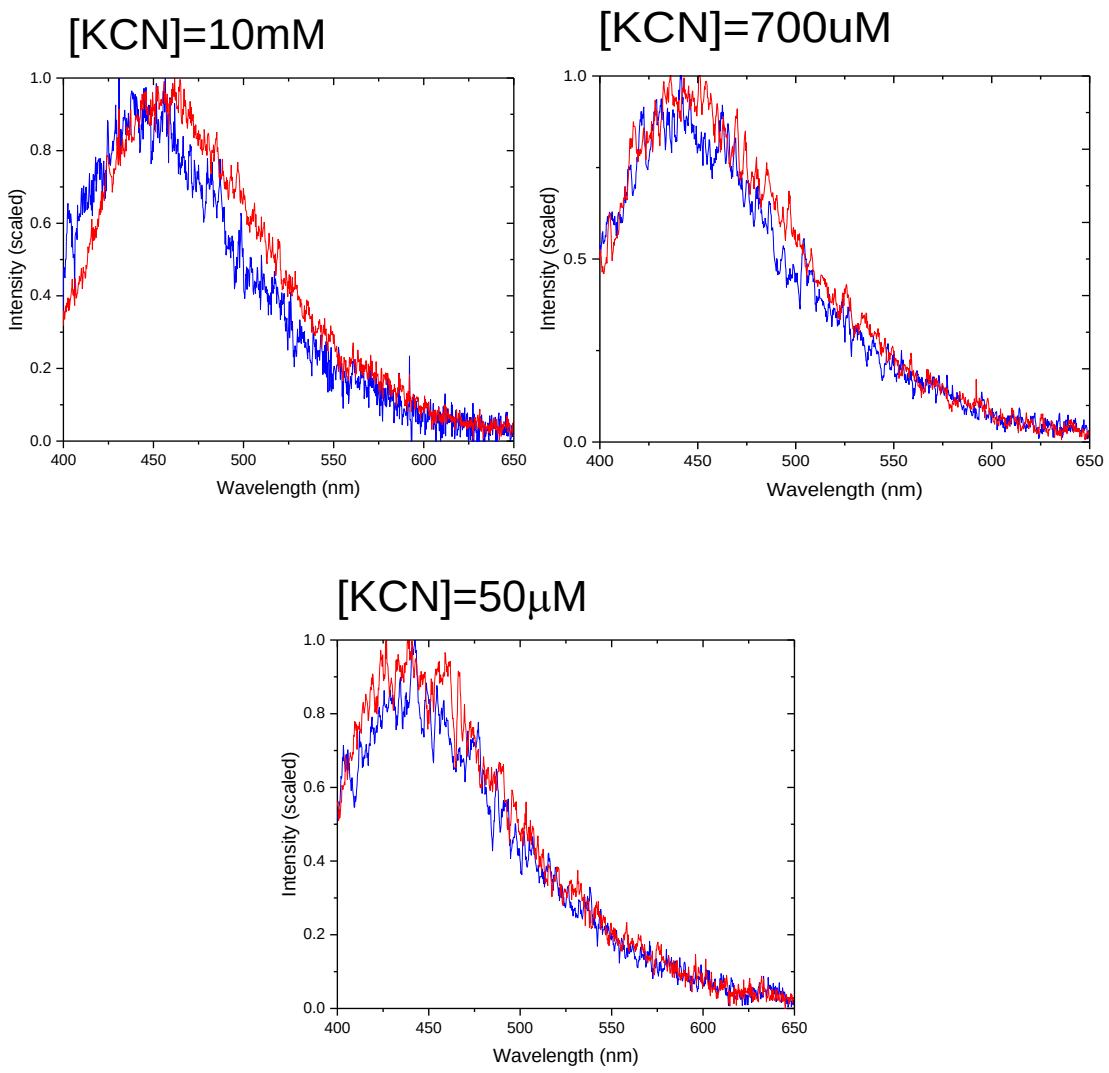


**Fig 3.1.4.2:** Emission spectrum before and after addition of cyanide. The blue spectrum is before cyanide added and the red spectrum is after cyanide added.

### 3.2 Autofluorescence Response with Various Concentrations of Cyanide (D-glucose)

#### 3.2.1 Autofluorescence Intensity vs. Time

In the second part of my experiment, both D-glucose and cyanide are added in the same trial. D-glucose is added in a concentration of 3mM to each sample, and we have used the same range of cyanide concentrations as in part one. We also have used same conditions which are added from the fifty times more concentrated stock solution of cyanide. In each case, we display the intensity vs. time for the additions of D-glucose and cyanide (See figure 3.2.1.1). We describe both full and late gate responses with the intensity vs. time measurements. We have observed many responses, both full and late gates have tracked each other almost exactly, the intensity vs. time plot also goes up when we add KCN, but there is an immediate increase followed by a gradual increase rather than decrease as seen with no glucose. Also, the largest intensity increase is with the highest cyanide concentration, and the intensity increase becomes smaller as the concentration of cyanide decreases. Moreover, the last point is that the amount of intensity increase is less than with no glucose. Like part one of the experiment, we also did four measurements on independent samples for each cyanide concentration with the added glucose (See Appendix for all data sets).

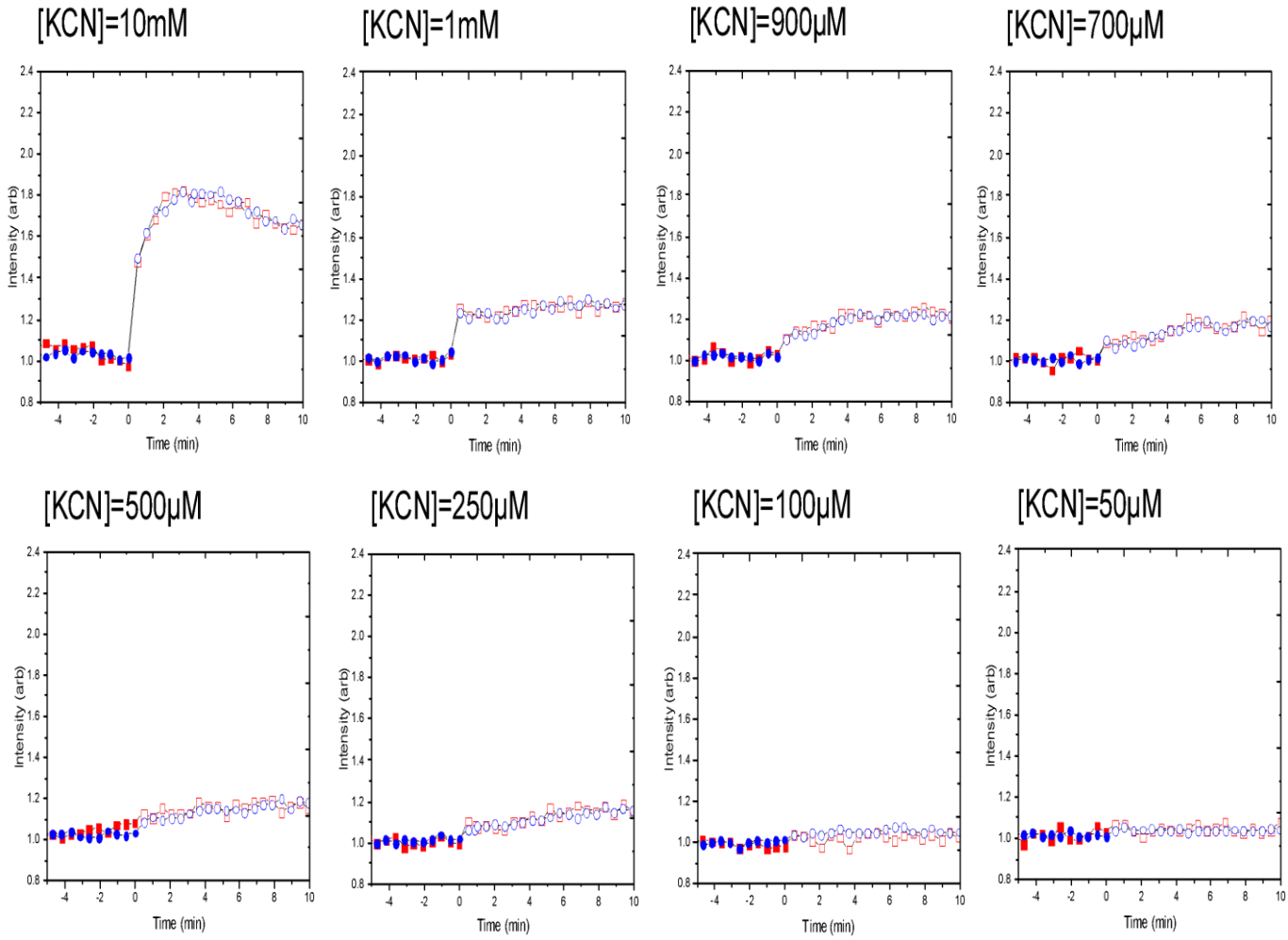


**Fig 3.2.1.1:** Monitoring autofluorescence response to D-glucose and cyanide additions. In all figures, full gate data are blue circles, and late-gate data are red squares. Each data point is a spectrally integrated intensity versus time, normalized to the intensity prior to chemical addition (Cyanide). Filled symbols are before cyanide addition and open symbols are after cyanide addition. Similarly, figures are shown on the (top) for addition of 10mM, 1mM, 900µM and 700µM cyanide. On the bottom, 500µM, 250µM, 100µM, and 50µM of cyanide. In all experiments, 3mM D-glucose was added 15mins prior to adding cyanide.

Further we have noticed the increase of intensity goes up with high concentrations of cyanide added in case of D-glucose used (See figure 3.2.1.2). It is significant to observe the difference between the full and late gate exponential lines of best fit are in better agreement in the trials with added glucose than without added glucose. On the other hand, from looking at the figure 3.2.1.2 we have observed that as an empirical fit, the exponential function has moved to the right side (after the concentration of cyanide 1mM) because the increase of intensity starts to go up 20mM to be more stable level of increase.

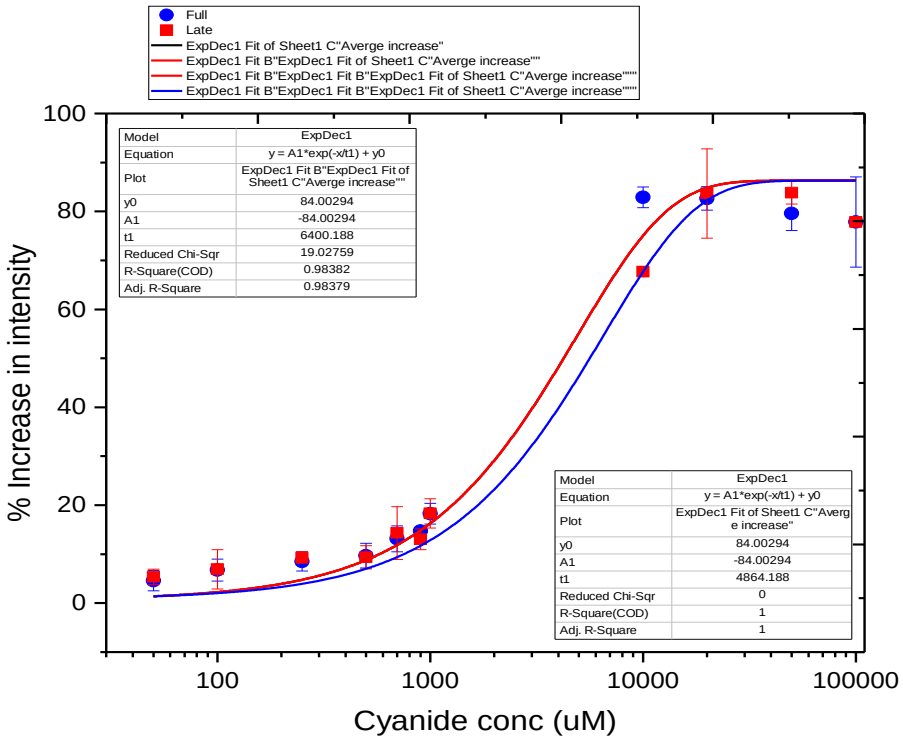


**Fig 3.2.1.2:** Percentage in intensity vs concentration of d-glucose and cyanide added. Red filled circles are shown late gate data and the blue filled squares are shown full gate data.

### 3.2.2 Discussion of Intensity vs. Time

In the second part of my experiment, we added D-glucose and cyanide to each sample. We also observe that the intensity goes up, for each concentration of cyanide added. But, we have noticed that the increase of intensity after KCN added, it almost has same increase percentage of the full and late gate. This is because D-glucose is the source of material for NADH production pathway in cellular respiration. Therefore, the pathways by which NADH is generated in the cytoplasm and Krebs cycle will be faster, thus it will result in more NADH production. We have been looking to free and protein-bound NADH forms as full measurement and the protein-bound NADH form as late measurement. Thus, there is no lag between full and late gate measurements as change from each other. If the pathway of generation of NADH in the cytoplasm and Krebs cycle is more active, then the mechanism by which free NADH is converted to protein-bound NADH should speed up. So, I think this is the reason behind why the intensity tracks more closely in autofluoresence intensity vs. time with various concentration of cyanide and D-glucose (See figure 3.2.2.1). We observe that the intensity goes up until the addition of KCN 10mM with glucose. Therefore, we can show evidence that D-glucose is able to counter the effect of cyanide action as an inhibitor limiting the effect of binding to complex IV in cellular of respiration (See figure 3.2.1.2).

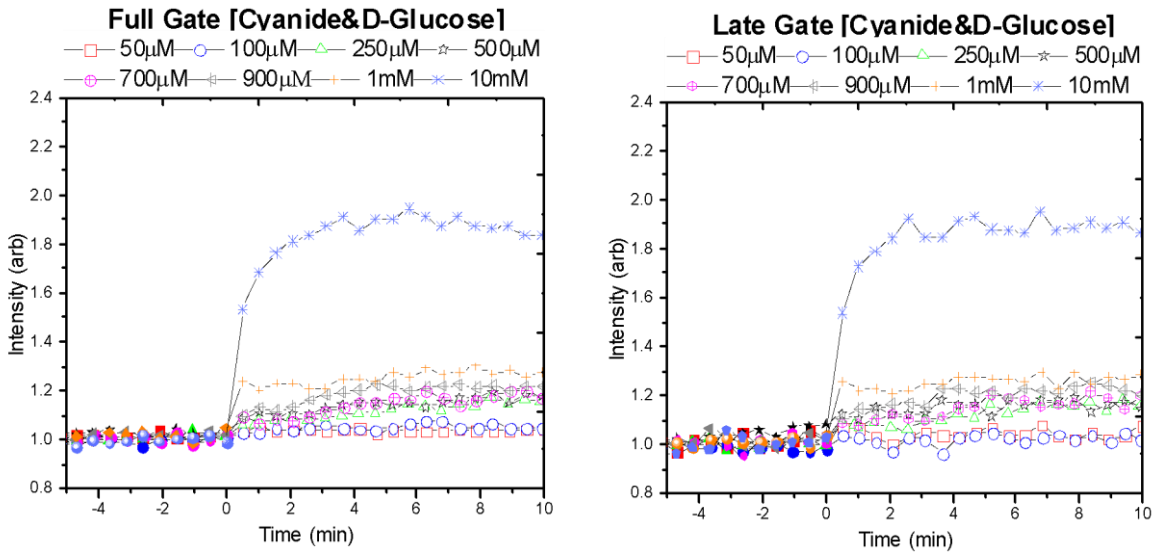


**Fig 3.2.2.1:** Monitoring autofluorescence response to cyanide additions. In the figure, full gate data, spectrally integrated intensity versus time, and late gate data, spectrally time-gated autofluorescence, normalized to the intensity prior to chemical addition (Cyanide). Autofluorescence spectra filled symbol (before cyanide addition) and open symbol (after cyanide addition). Similarly, figures are shown on the (Left) full gate data and on the (Right), late gate data for addition of 10mM, 1mM, 900µM, 700µM, 500µM, 250µM, 100µM and 50µM of cyanide. 3mM D-glucose addition and different concentrations of cyanide.

### 3.2.3 Spectral Phasor Analysis

Using the spectral phasor technique, we see differences with the addition of D-glucose and cyanide concentrations in path directions and positions when compared to the trials without added glucose. We do not see a difference in the shift direction in the low cyanide concentrations like in the trails without added glucose. However, in the trails with added glucose we see a positive shift in both the real and imaginary axis for the late gate (See figure 3.2.3.1). We made the spectral phasor plot which shows the position increases in the highest cyanide concentrations while in the lowest concentrations decrease depending on amount addition of cyanide concentration. We have further noticed that at high cyanide concentrations clear shift are observed for the full (blue) and late gate (red). Moreover, at the low cyanide concentrations we

continue to observe that full and late gate positive shift a little in imaginary and real direction. For example, the lowest concentrations of KCN in the real axis start to see the positive values.

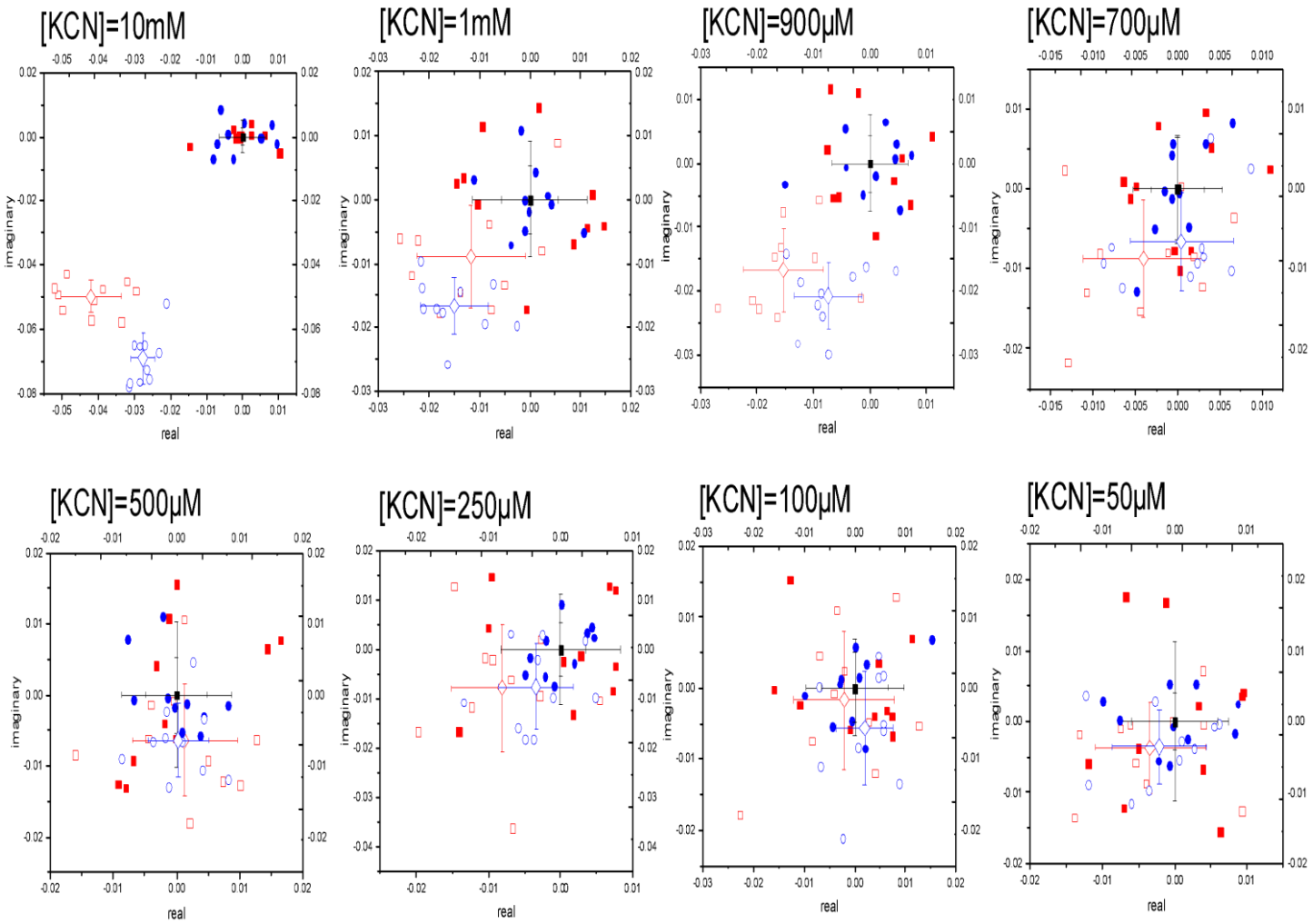


**Fig 3.2.3.1:** Spectral phasor plots for different concentration to D-glucose and cyanide added. In all figures, full gate data are blue circles, and late-gate data are red squares. Each data point is a spectrally integrated intensity versus time, normalized to the intensity prior to chemical addition (Cyanide). Filled symbols are before cyanide addition and open symbols are after cyanide addition. Similarly, figures are shown on the (top) for addition of 10mM, 1mM, 900µM and 700µM cyanide. On the bottom, 500µM, 250µM, 100µM, and 50µM of cyanide. In all experiments, 3mM D-glucose was added 15mins prior to adding cyanide.

### 3.2.4 Discussion of Spectral Phasor Analysis

Applying the spectral phasor analysis to the experiments with the addition of D-glucose and cyanide allows the investigation into whether the observed different responses are consistent with a two-state model. In each experiment, we monitor the spectral phasor plot as detected by both the full and late measurements. In the figures the imaginary and real axis are shifted so that both full and late gates are zero when the cyanide is added (See figure 3.2.3.1). Like in the case where only cyanide was added, we have observed that the phasor shift is shown to be in a similar direction, however the late gate shift gets more positive in the imaginary and real directions at the low cyanide concentrations such as 50μM,100μM and 250μM (See figure 3.2.4.1). Since the phasor points depend on spectrum shape from each sample, we have more information about the dynamics of NADH conformations. This point is very important to help us understand the metabolic activity during respiration inside the cells because the shifts of positions in spectral phasor technique depends on the changes in the peak or/and width of spectrum shape after cyanide added.

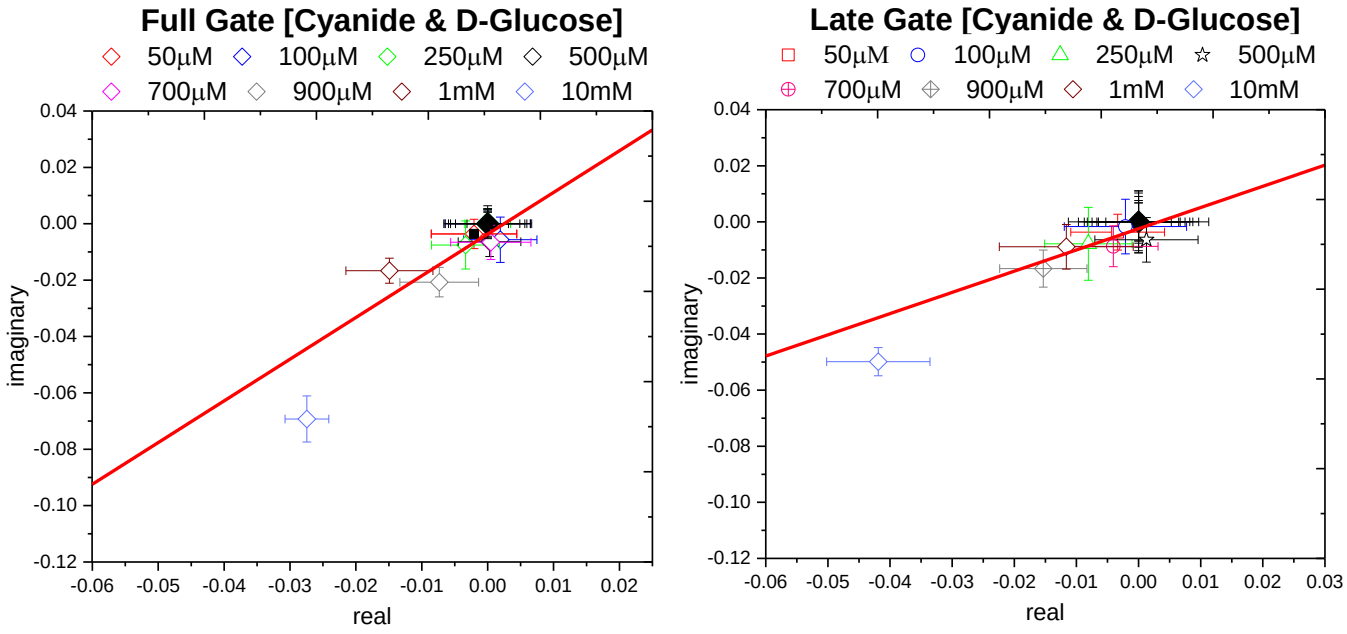


**Fig 3.2.4.1:** Spectral phasor plots for different concentration to D-glucose and cyanide added. In the figure, full gate data, spectrally integrated intensity versus time, and late gate data, spectrally time-gated autofluorescence, normalized to the intensity prior to chemical addition (Cyanide). Autofluorescence spectra filled symbol (before cyanide addition) and open symbol (after cyanide addition). Similarly, figures are shown on the (Left) full gate data and on the (Right) late gate data for addition of 10mM, 1mM, 900µM, 700µM, 500µM, 250µM, 100µM and 50µM of cyanide. 3mM D-glucose addition and different concentrations of cyanide.

To verify that the plot of spectral phasor components calculated from Gaussian shaped, which is coming from two components lie along a line, before and after addition of concentration cyanide. Gaussian shaped says, the width of the spectrum increases, the spectral points gradually move from zero to infinity (to center). Thus, it applies on the concentration of cyanide 50µM, 700µM and 10mM where the width of the spectrum increases (See figure 3.2.4.2).

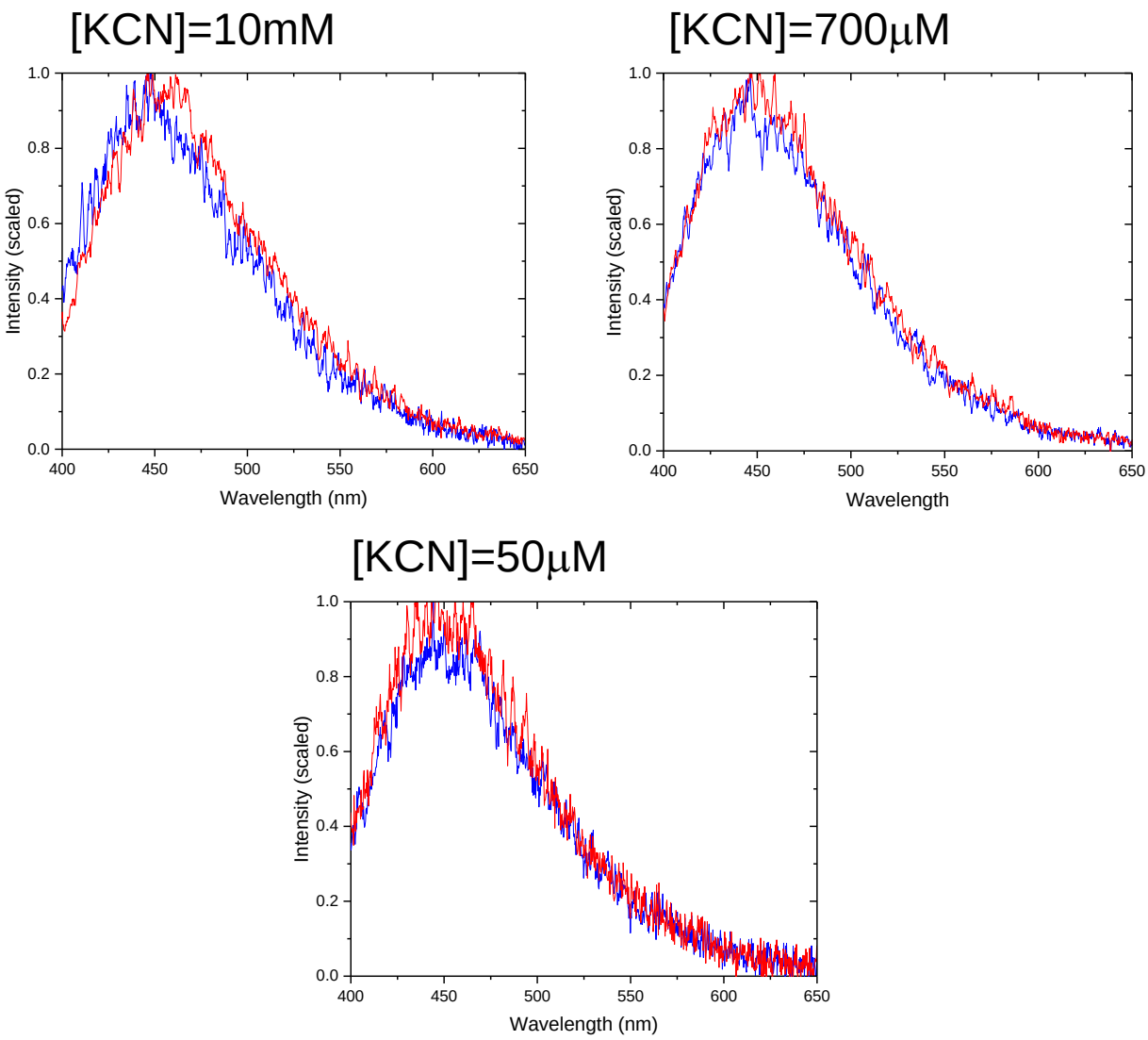


**Fig 3.2.4.2:** Emission spectrum before and after addition of cyanide and D-glucose. The blue spectrum is before cyanide added and the red spectrum is after cyanide added.

### 3.3 Additional Discussion

Previous researchers showed that cyanide binds respiration (cytochrome c oxidase), and these studies showed that the oxygen consumption measurements have different responses at low and high concentrations of cyanide. Such as:

- Eraldo Antonini, et al. formulated a ratio between the rate of oxidation by cytochrome c oxidase and the addition of different concentrations of cyanide. They said, "It is apparent that the velocity of oxidation is decreased more and more as the concentration of cyanide is increased" [24].
- Heather B. Leavesle et al. have explained that cyanide inhibits cellular oxygen consumption. They showed "KCN produced a concentration- dependent inhibition of complex IV for 2-60μM concentration range. And cyanide's medium inhibitory concentration was estimated at $13.2 \pm 1.8$μM KCN" [4].

These scientists studied the effect of cyanide on cellular oxygen consumption, but there are other effects of cyanide that one can study such as mitochondrial membrane potential (proton transport) and the enzyme affinity to oxygen [5, 13]. Although cyanide has three main effects on mitochondrial function, we study them indirectly via its effect on NADH fluorescence. The effect of cyanide is dependent on its cellular concentration.

My data shows that we have been able to study the concentration dependence of cyanide action, and we have compared this dependence between two projects (glucose and no glucose). Firstly, in both the glucose and no-glucose trials we noticed that the intensity increases when the cyanide is added. The largest intensity increase is with the highest cyanide concentration, and the intensity increase becomes smaller as the concentration of cyanide decreases. In the no glucose trials, the amount of full gate (blue) intensity vs. time increased more than the late gate (red) trials. In the trials with glucose the full and late gate intensity vs. time are almost same percentage because the D-glucose is the source of material for NADH production pathway in cellular respiration. Therefore, these pathways in the cytoplasm and Krebs cycle will be faster, thus the reduction of NADH will be more stimulated (See figure 3.1.2.1, 3.2.2.1, and 3.3.1). For example, the proportion of percentage increase in intensity full gate after cyanide added 10mM is 54.73%, while in the addition D-glucose and cyanide is 44.54% etc. But, in the late gate, it

further shows a difference of response in cyanide added such as 250μM is 19% and in D-glucose and cyanide added is 7.99% (See table 3.3.1). Thus, the responses of percentage increase of intensity go down through using the D-glucose added depending on cyanide action.

**Table 3.3.1:** The percentage increase in intensity full and late gates for addition of cyanide and D-glucose.

| Concentration of KCN | Percentage increase in intensity (Full) After Cyanide | Percentage increase in intensity (Full) After Cyanide & D-glucose | Percentage increase in intensity (Late) After Cyanide | Percentage increase in intensity (Late) After Cyanide & D-glucose |
|---|---|---|---|---|
| 50μM | 1.69 % | 2.31 % | 0.93 % | 2.92 % |
| 100μM | 5.91 % | 4.31 % | 5.35 % | 2.7 % |
| 250μM | 23.47 % | 6.93 % | 19 % | 7.99 % |
| 500μM | 29.02 % | 8.59 % | 25.34 % | 8.06 % |
| 700μM | 32.64 % | 9.7 % | 27.16 % | 10.04 % |
| 900μM | 35.21 % | 12.74 % | 22.97 % | 13.38 % |
| 1mM | 39.68 % | 17.63 % | 31.31 % | 18.53 % |
| 10mM | 54.73 % | 44.54 % | 44.76 % | 44.7 % |

Additionally, we show an exponential increase in intensity with increasing cyanide concentrations. However, we go beyond in our study by having both full and late measurements (See figure 3.1.1.2). We have observed the intensity increase goes up with increased concentrations.

In both glucose and no-glucose cases, we made spectral phasor plots which showed clear shifts at high cyanide concentrations for both the full (blue) and late gate (red). While, at the lower cyanide concentrations we observed a decrease in shift in both the full and late gate. In the trials without added glucose, the samples with the highest concentrations of KCN show clear shifts in the imaginary axis, and in the lowest concentrations we start to see a change in shift direction. In general, the shift in the full and late gate decreases and gets more negative in the real and imaginary directions with full gate shifts more so in the imaginary, and this trend continues until at low concentrations when the shift changes direction. But, in the trials with added glucose, we have also noticed clear shifts at high cyanide concentrations for the full and

late gate. Moreover, at the low cyanide concentrations we also continue to observe that full and late gate shifts change a little in direction. For example, the lowest concentrations of KCN in the real axis we start to see the positive values (See figures 3.1.4.1, 3.2.4.1).

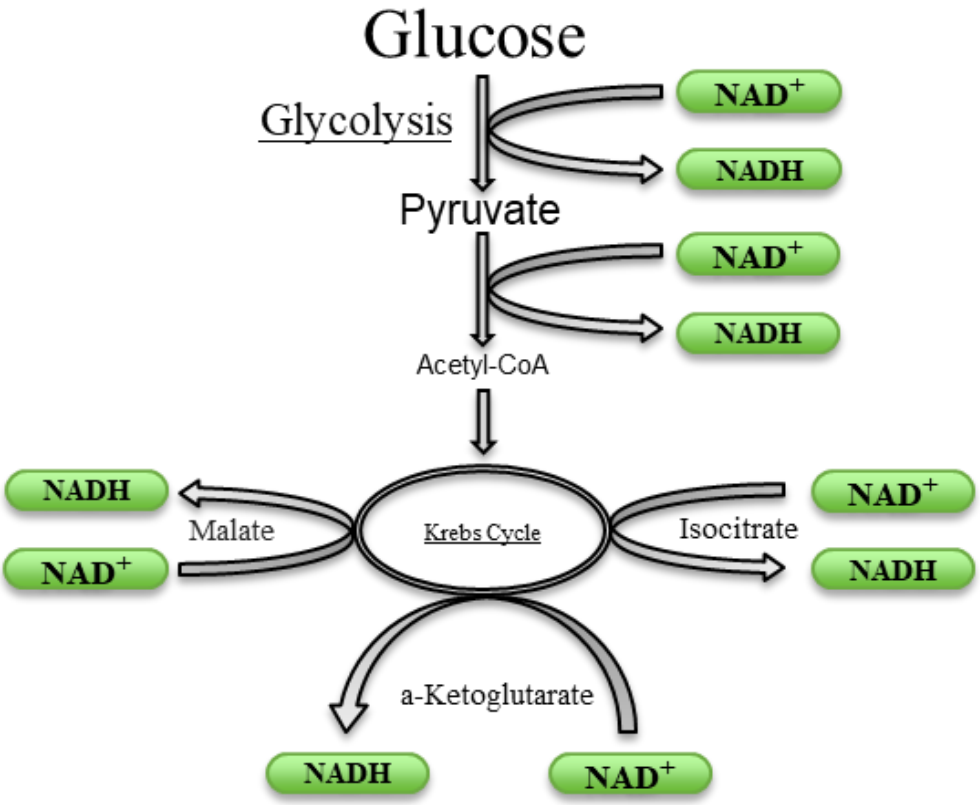


**Fig 3.3.1:** Showing the reduction of $NAD^+$ to NADH.

Comparing my results to the work of a previous graduate student (Gaire) within the lab, we find my data to be consistent using the spectral phasor technique. The left slide (my data) has better contrast than Gaire's data using spectral phasor detection [23]. Our data points are very consistent in terms of average positions and directions across a range of concentrations of cyanide added. Thus, this suggests that our data is accurate. Using the spectral phasor detection, we can visualize the ability to identify the small changes in cyanide responses at the low concentrations (See figure 3.3.2).

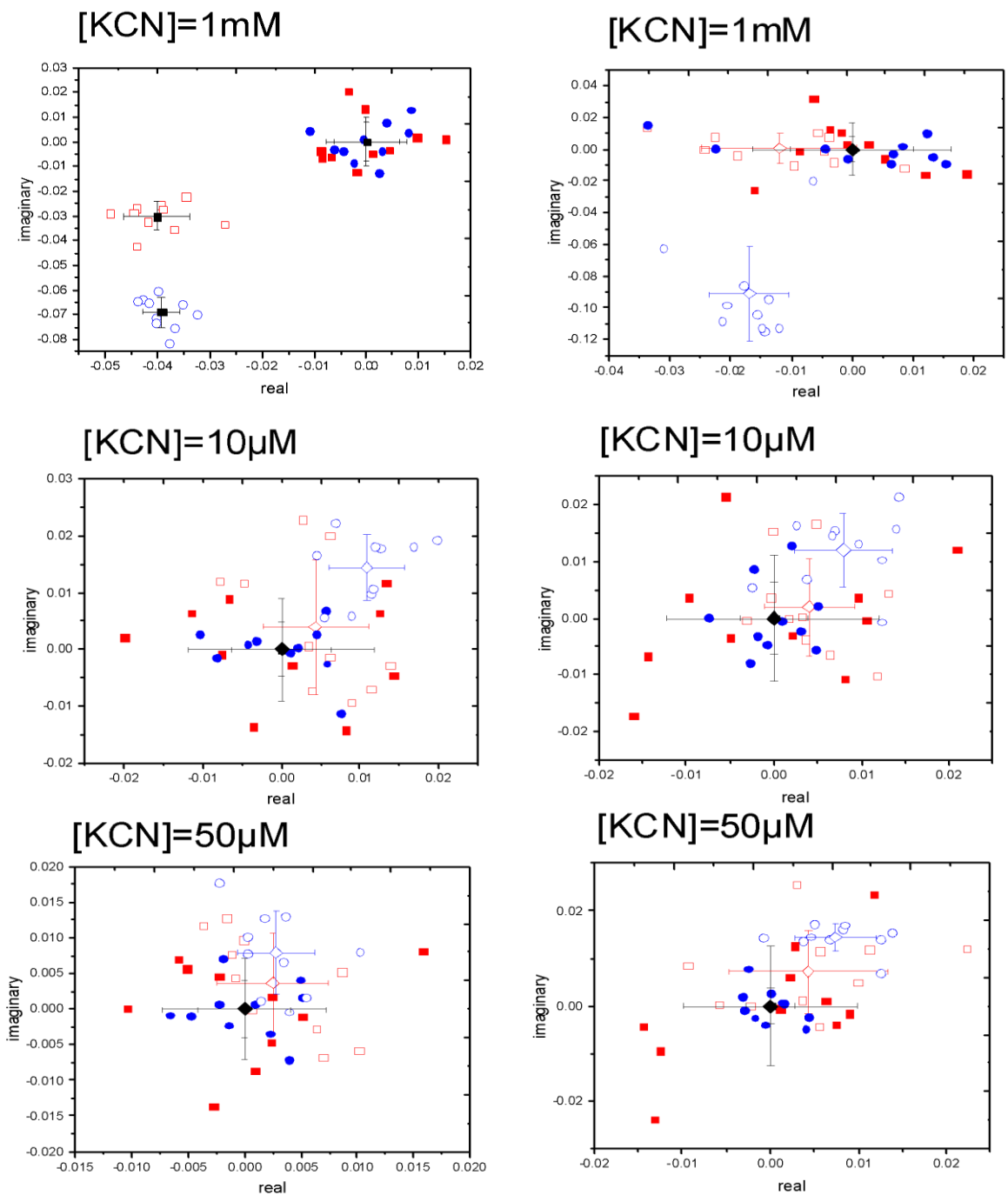


**Fig 3.3.2:** Spectral phasor plots for different concentration of cyanide added. In the figure, full gate data, spectrally integrated intensity versus time, and late gate data, spectrally time-gated autofluorescence, normalized to the intensity prior to chemical addition (Cyanide). Autofluorescence spectra filled symbol (before cyanide addition) and open symbol (after cyanide addition). Similarly, figures are shown on the (left) Nazar data. But, figures are shown on the (right) Madhu data.

# Chapter 4
# Conclusions and Future Work

## 5.1 Conclusions

In my introduction, I proposed two goals for this thesis. I would like to revisit these and state my conclusions.

**I.** My first goal was to establish a relationship between autofluorescence spectrum shape change and the concentration of cyanide added. After completion of many experiments and analyzing my data, I have confirmed that the intensity increases with an increasing cyanide concentration. Also, the intensity increase of full and late gates are different dynamic. For example, in 10mM of full gate measurement increases more than late gate because it measures the free and protein-bound NADH. The different direction and amount shift of the spectral phasor point is indicative of a different mitochondrial pathway being affected. The spectral phasor analysis detects different responses at low cyanide concentrations, specifically in the 50μM and 10μM samples (See figure 5.4.1). But, in the highest cyanide concentrations, we start to lose collinearity, our indication for two state behavior. This suggests that higher concentrations of cyanide effect different metabolic activities than do the lower concentrations. Further, we have shown that NADH conformational changes measured by autofluorescence spectrum shape can be a useful technique for the detection of cellular metabolic system differences that is both real-time and non-invasive.

**II.** The second objective in this thesis was to investigate the effects of both added D-glucose and cyanide to our sample. My data demonstrates that when D-glucose is added with cyanide to cellular samples we see the amount of intensity increase decreases when D-glucose is added along with cyanide to the sample. The process of D-glucose and cyanide is explained in chapters 1 and 3, the intensity increase of full and late gates are same dynamic (See figure 3.2.1.1). Additionally, the amount of phasor space shift decreases when analyzing the spectra with the spectral phasor technique with the addition of D-glucose (See figures 3.2.4.1-3.2.2.1). Thus, the addition of D-glucose to the sample counters cyanide's effect as a chemical to perturb the cell's metabolism.

## 5.2 Future Work

An interesting extension of my data will be acquiring data using cyanide concentrations outside the range presented here in my thesis. There is still more work to be done to solidify the trends shown in my data, such as additional measurements for added cyanide in concentrations less than 50μM to be more confident about the change in direction of the spectral shift. Also, taking data for added cyanide concentrations above 10mM could confirm the departure from a collinear trend that my data suggests, strengthening our conclusions about the concentration dependence of cyanide action.

Another point is that the intensity change for the autofluorescence spectra of NADH are different percentages between the trials with and without added glucose. Thus, it will be very interesting to repeat similar metabolic experiments described in the previous chapter with added glucose. An example of such experiments could be to take data using many glucose concentrations to better analyze the effects of glucose on cyanide as an inhibitor of cellular reparation.

Also, our lab is interested in studying the effects of high pressure on cellular metabolic responses. It will be interesting to take similar data presented in this thesis using our lab's high-pressure system to study how pressure effects the metabolic response to cyanide.

## Reference


[1] B. Alberts, *Molecular biology of the cell*. Garland Pub, 1994.

[2] L. Stryer, *Biochemistry*. W.H. Freeman, 1988.

[3] A. A. Heikal, "Intracellular coenzymes as natural biomarkers for metabolic activities and mitochondrial anomalies," *Biomark. Med.*, vol. 4, no. 2, pp. 241–263, 2010.

[4] H. B. Leavesley, L. Li, K. Prabhakaran, J. L. Borowitz, and G. E. Isom, "Interaction of cyanide and nitric oxide with cytochrome c oxidase: Implications for acute cyanide toxicity," *Toxicol. Sci.*, vol. 101, no. 1, pp. 101–111, 2008.

[5] B. M. Bakker *et al.*, "Stoichiometry and compartmentation of NADH metabolism in Saccharomyces cerevisiae," *FEMS Microbiol. Rev.*, vol. 25, no. 1, pp. 15–37, 2001.

[6] S. A. Siano and R. Mutharasan, "NADH and flavin fluorescence responses of starved yeast cultures to substrate additions," *Biotechnol. Bioeng.*, vol. 34, no. 5, pp. 660–670, Aug. 1989.

[7] A. Barrientos, "Yeast Models of Human Mitochondrial Diseases," *IUBMB Life*, vol. 55, no. 2, pp. 89–95, 2003.

[8] J. De Ruyck, M. Famerée, J. Wouters, E. A. Perpète, J. Preat, and D. Jacquemin, "Towards the understanding of the absorption spectra of NAD(P)H/NAD(P)+ as a common indicator of dehydrogenase enzymatic activity," *Chem. Phys. Lett.*, vol. 450, no. 1–3, pp. 119–122, 2007.

[9] "biochemistry - Why does NADH have 2 peaks in its absorption spectrum but NAD+ has only one? - Chemistry Stack Exchange." .

[10] J. R. Lakowicz, "3. Fluorophores," *Princ. Fluoresc. Spectrosc.*, p. 954, 2009.

[11] Z. Long *et al.*, "The real-time quantification of autofluorescence spectrum shape for the monitoring of mitochondrial metabolism," *J. Biophotonics*, vol. 8, no. 3, pp. 247–257, 2015.

[12] J. Maltas *et al.*, "Autofluorescence from NADH conformations associated with different metabolic pathways monitored using nanosecond-gated spectroscopy and spectral phasor analysis," *Anal. Chem.*, vol. 87, no. 10, pp. 5117–5124, 2015.

[13] U. Kalnenieks, N. Galinina, M. M. Toma, and R. K. Poole, "Cyanide inhibits respiration yet stimulates aerobic growth of Zymomonas mobilis," *Microbiology*, vol. 146, no. 6, pp. 1259–1266, 2000.

[14] H. Nůsková, M. Vrbacký, Z. Drahota, and J. Houštěk, "Cyanide inhibition and pyruvate-induced recovery of cytochrome c oxidase," *J. Bioenerg. Biomembr.*, vol. 42, no. 5, pp. 395–403, 2010.

[15] A. A. Biradar, A. V. Biradar, T. Sun, Y. Chan, X. Huang, and T. Asefa, "Bicinchoninic acid-based colorimetric chemosensor for detection of low concentrations of cyanide," *Sensors Actuators, B Chem.*, vol. 222, pp. 112–119, 2016.

[16] Y. Weihai, “NAD+/NADH and NADP+/ NADPH in Cellular Functions and Cell Death: Regulation and Biological Consequences.” San Francisco, University of California.

[17] G. H. Patterson, S. M. Knobel, P. Arkhammar, O. Thastrup, and D. W. Piston, “Separation of the glucose-stimulated cytoplasmic and mitochondrial NAD(P)H responses in pancreatic islet beta cells.,” *Proc. Natl. Acad. Sci. U. S. A.*, vol. 97, no. 10, pp. 5203–5207, 2000.

[18] “Difference Between D and L Glucose | D vs L Glucose.” [Online]. Available: http://www.differencebetween.com/difference-between-d-and-vs-l-glucose/. [Accessed: 11-Jan-2018].

[19] Z. Long *et al.*, “The real-time quantification of autofluorescence spectrum shape for the monitoring of mitochondrial metabolism,” *J. Biophotonics*, vol. 8, no. 3, pp. 247–257, Mar. 2015.

[20] A. H. A. Clayton, Q. S. Hanley, and P. J. Verveer, “Graphical representation and multicomponent analysis of single-frequency fluorescence lifetime imaging microscopy data,” *J. Microsc.*, vol. 213, no. 1, pp. 1–5, 2004.

[21] C. Stringari, A. Cinquin, O. Cinquin, M. A. Digman, P. J. Donovan, and E. Gratton, “Phasor approach to fluorescence lifetime microscopy distinguishes different metabolic states of germ cells in a live tissue,” *Nat Acad Sci Proc*, vol. 108, no. 33, pp. 13582–13587, 2011.

[22] F. Fereidouni, A. N. Bader, and H. C. Gerritsen, “Spectral phasor analysis allows rapid and reliable unmixing of fluorescence microscopy spectral images,” *Opt. Express*, vol. 20, no. 12, p. 12729, 2012.

[23] J. Maltas *et al.*, “Autofluorescence from NADH Conformations Associated with Different Metabolic Pathways Monitored Using Nanosecond-Gated Spectroscopy and Spectral Phasor Analysis,” *Anal. Chem.*, vol. 87, no. 10, pp. 5117–5124, May 2015.

[24] E. Antonini, M. Brunori, G. C. Rotilio, C. Greenwood, and B. G. MalmstrÖM, “The Interaction of Cyanide with Cytochrome Oxidase,” *Eur. J. Biochem.*, vol. 23, no. 2, pp. 396–400, 1971.

# Appendix

## KCN

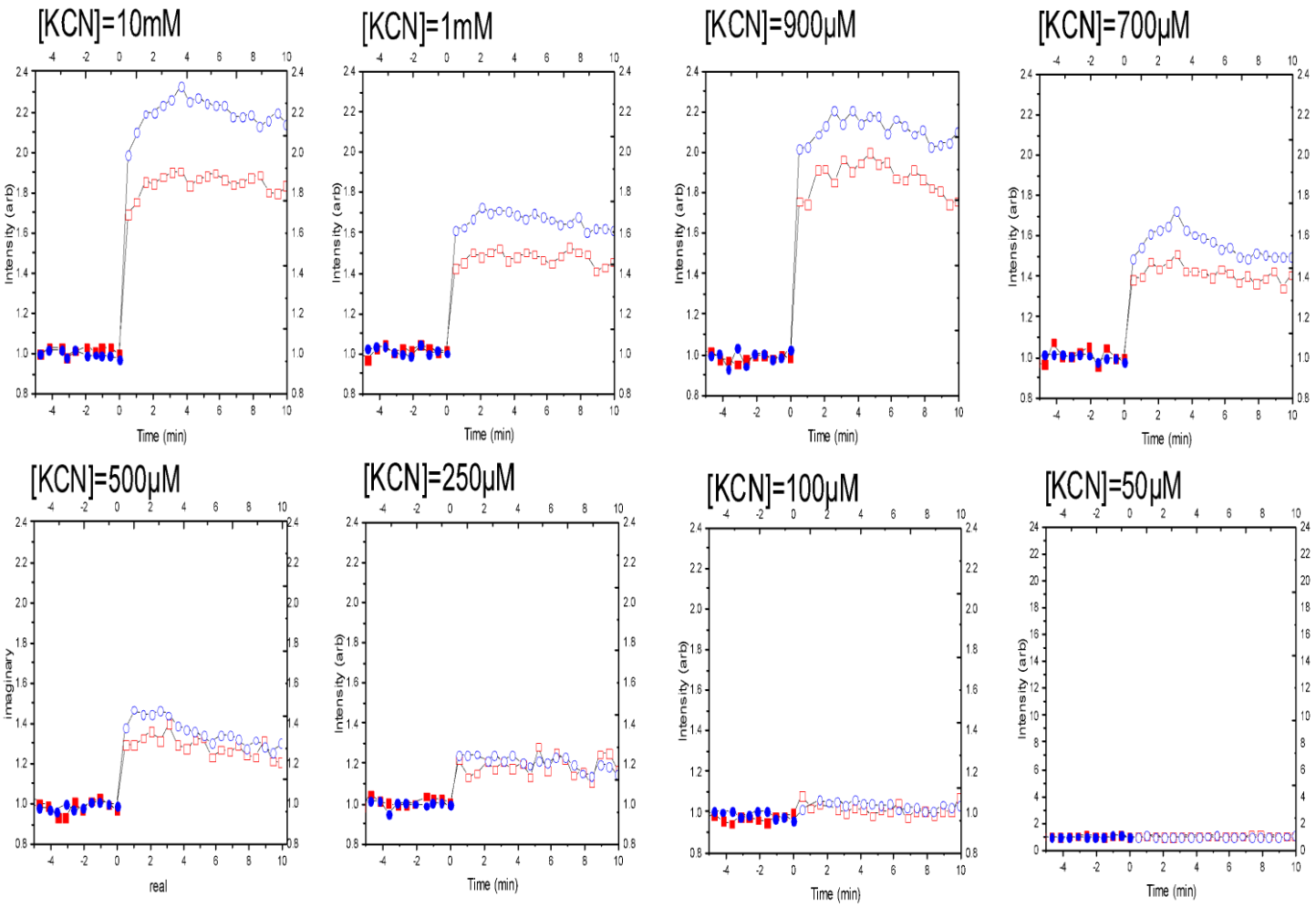


Monitoring autofluorescence response to cyanide additions. In all figures, full gate data are blue circles, and late-gate data are red squares. Each data point is a spectrally integrated intensity versus time, normalized to the intensity prior to chemical addition (Cyanide). Filled symbols are before cyanide addition and open symbols are after cyanide addition. Similarly, figures are shown on the (top) for addition of 10mM, 1mM, 900µM and 700µM cyanide. On the bottom, 500µM, 250µM, 100µM, and 50µM of cyanide.

# KCN

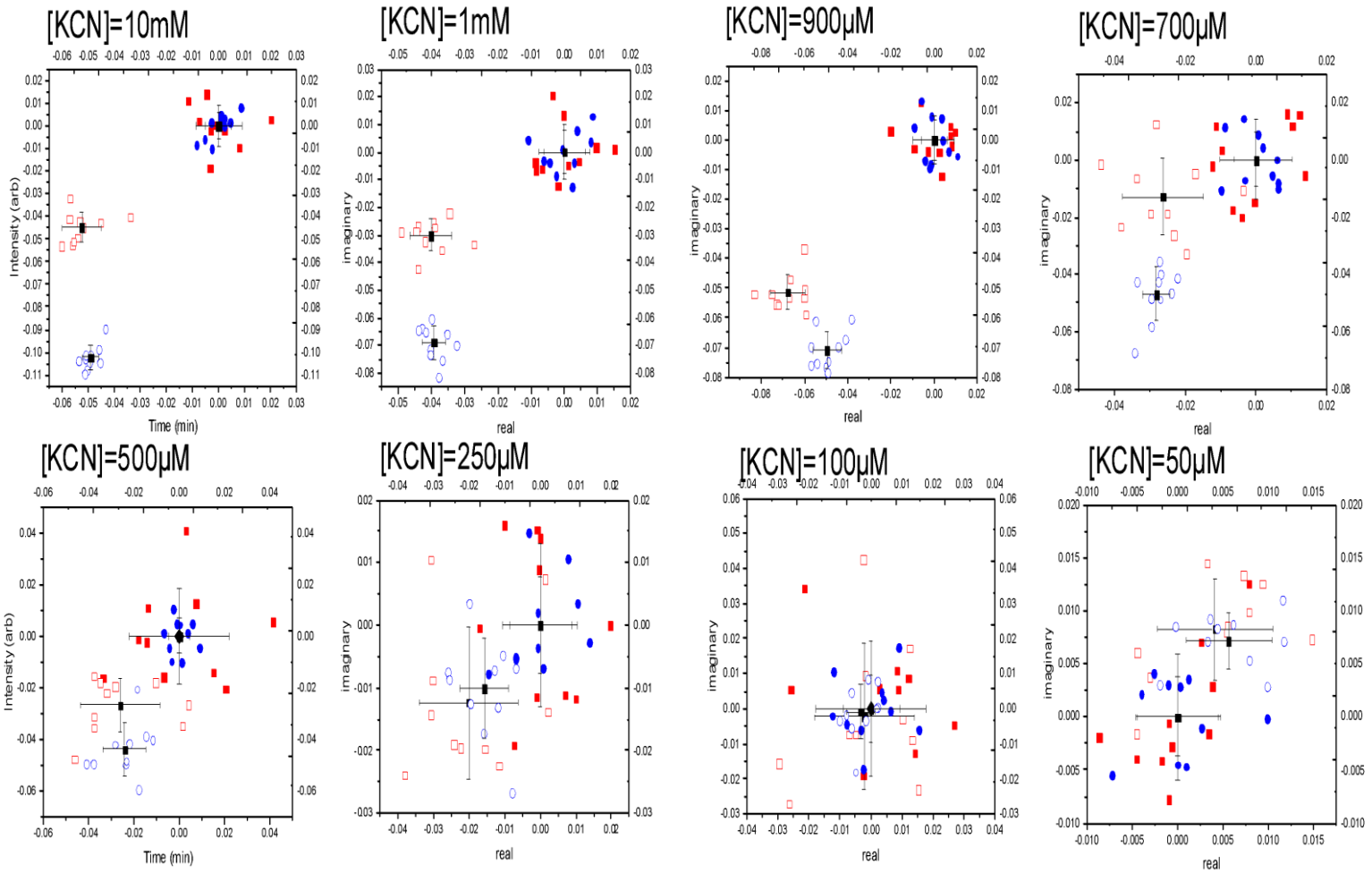


Spectral phasor plots for different concentration of cyanide added. In all figures, full gate data are blue circles, and late-gate data are red squares. Each data point is a spectrally integrated intensity versus time, normalized to the intensity prior to chemical addition (Cyanide). Filled symbols are before cyanide addition and open symbols are after cyanide addition. Similarly, figures are shown on the (top) for addition of 10mM, 1mM, 900µM and 700µM cyanide. On the bottom, 500µM, 250µM, 100µM, and 50µM of cyanide.

# KCN

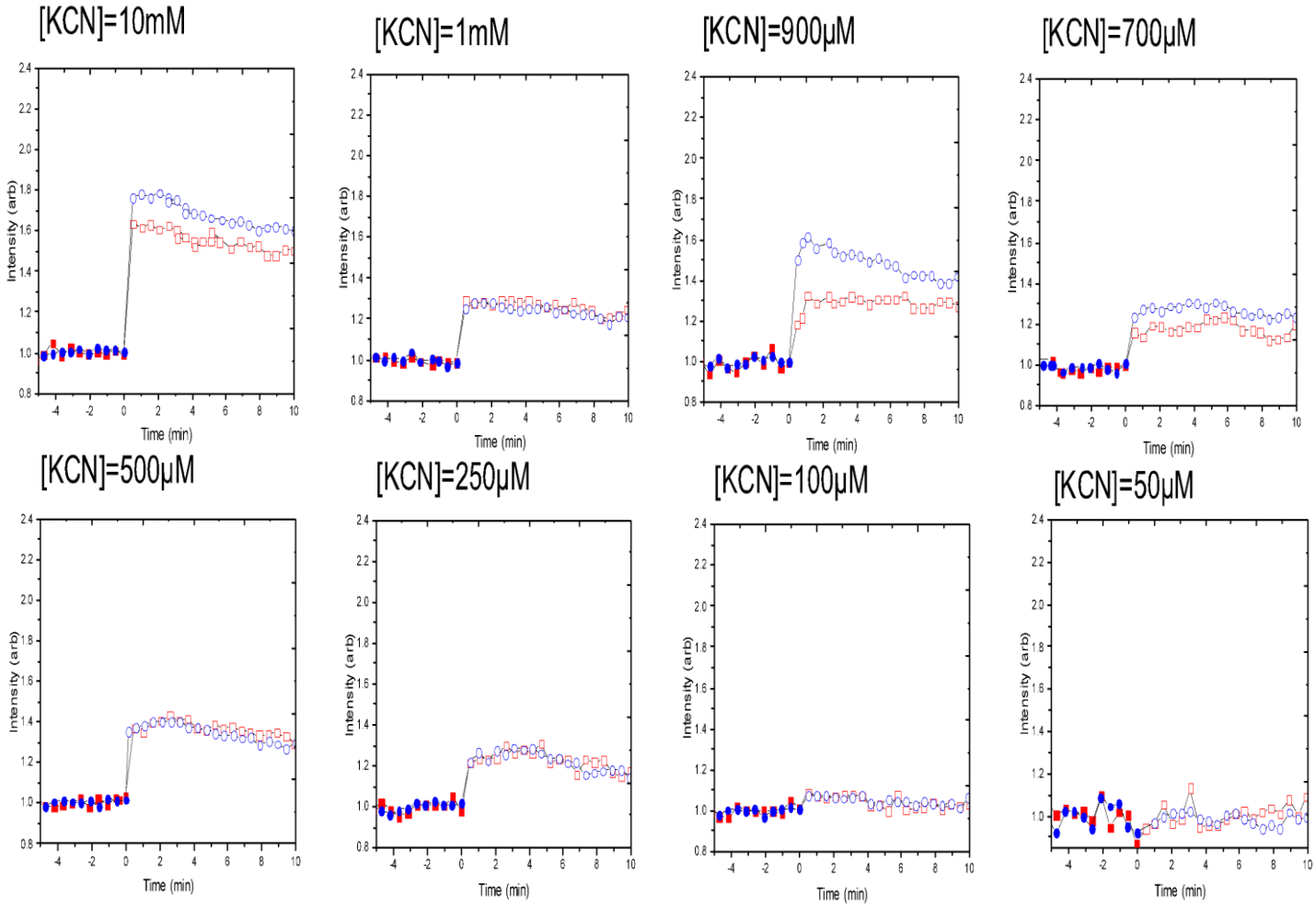


Monitoring autofluorescence response to cyanide additions. In all figures, full gate data are blue circles, and late-gate data are red squares. Each data point is a spectrally integrated intensity versus time, normalized to the intensity prior to chemical addition (Cyanide). Filled symbols are before cyanide addition and open symbols are after cyanide addition. Similarly, figures are shown on the (top) for addition of 10mM, 1mM, 900µM and 700µM cyanide. On the bottom, 500µM, 250µM, 100µM, and 50µM of cyanide.

# KCN

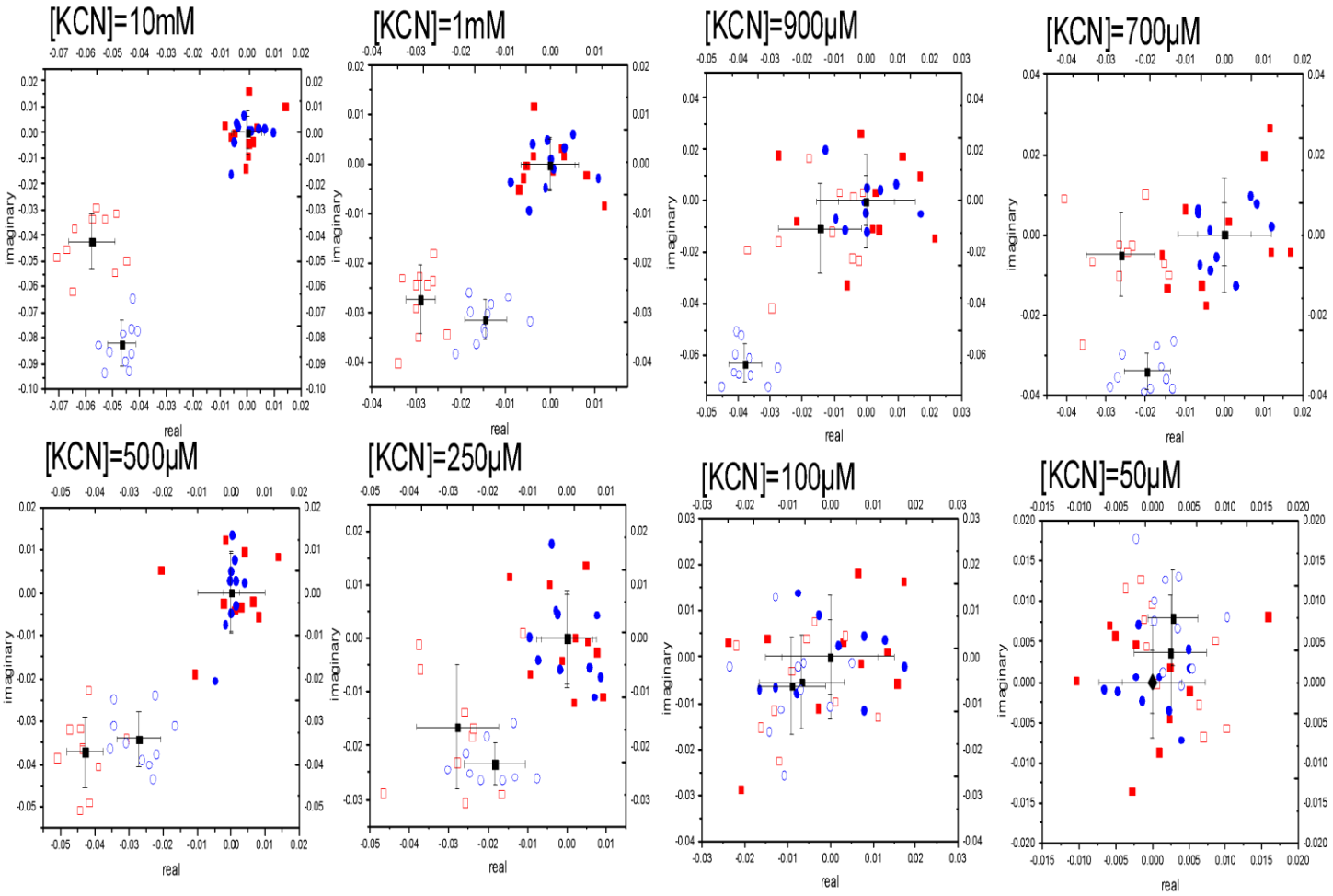


Spectral phasor plots for different concentration of cyanide added. In all figures, full gate data are blue circles, and late-gate data are red squares. Each data point is a spectrally integrated intensity versus time, normalized to the intensity prior to chemical addition (Cyanide). Filled symbols are before cyanide addition and open symbols are after cyanide addition. Similarly, figures are shown on the (top) for addition of 10mM, 1mM, 900µM and 700µM cyanide. On the bottom, 500µM, 250µM, 100µM, and 50µM of cyanide.

# KCN

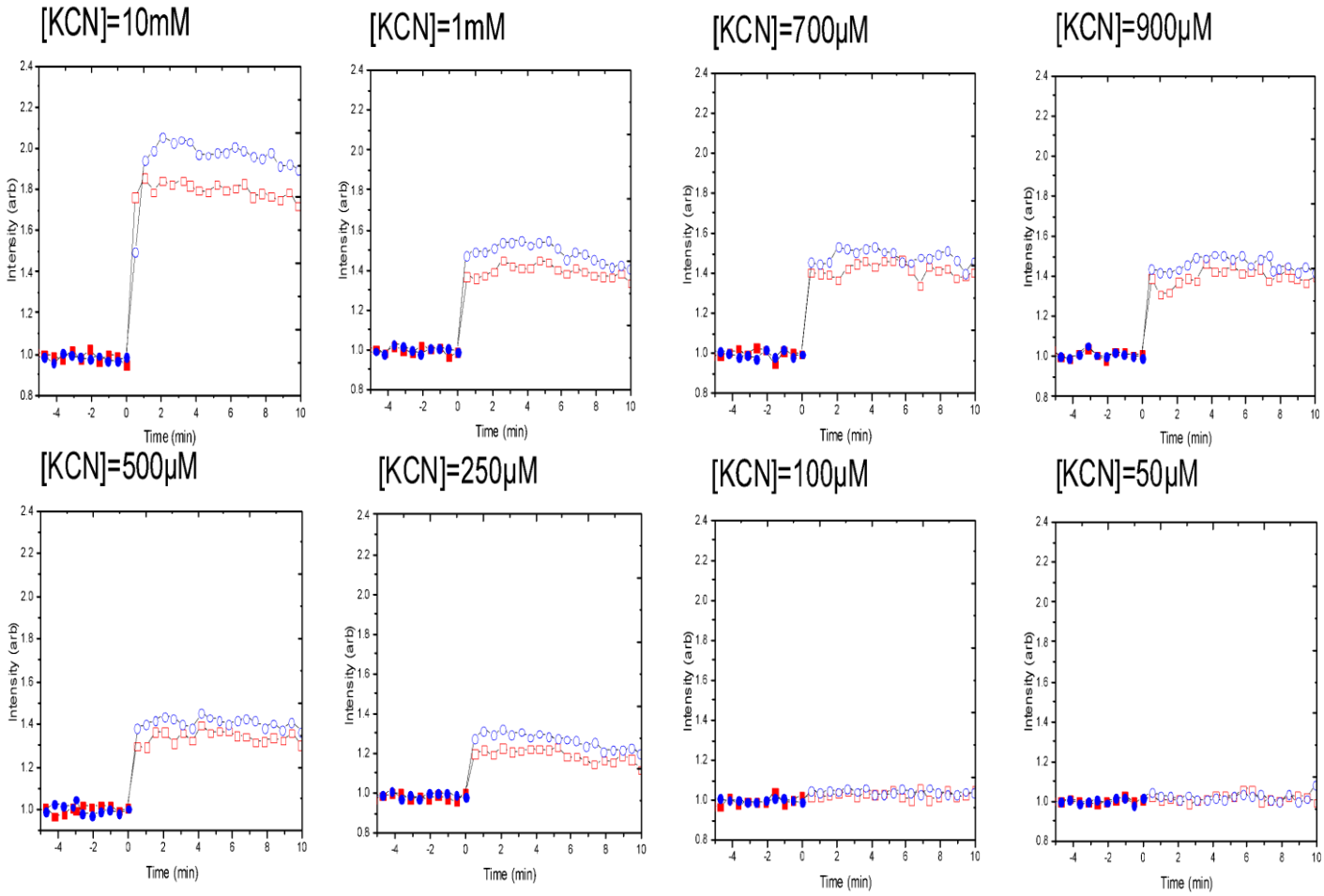


Monitoring autofluorescence response to cyanide additions. In all figures, full gate data are blue circles, and late-gate data are red squares. Each data point is a spectrally integrated intensity versus time, normalized to the intensity prior to chemical addition (Cyanide). Filled symbols are before cyanide addition and open symbols are after cyanide addition. Similarly, figures are shown on the (top) for addition of 10mM, 1mM, 900µM and 700µM cyanide. On the bottom, 500µM, 250µM, 100µM, and 50µM of cyanide.

# KCN

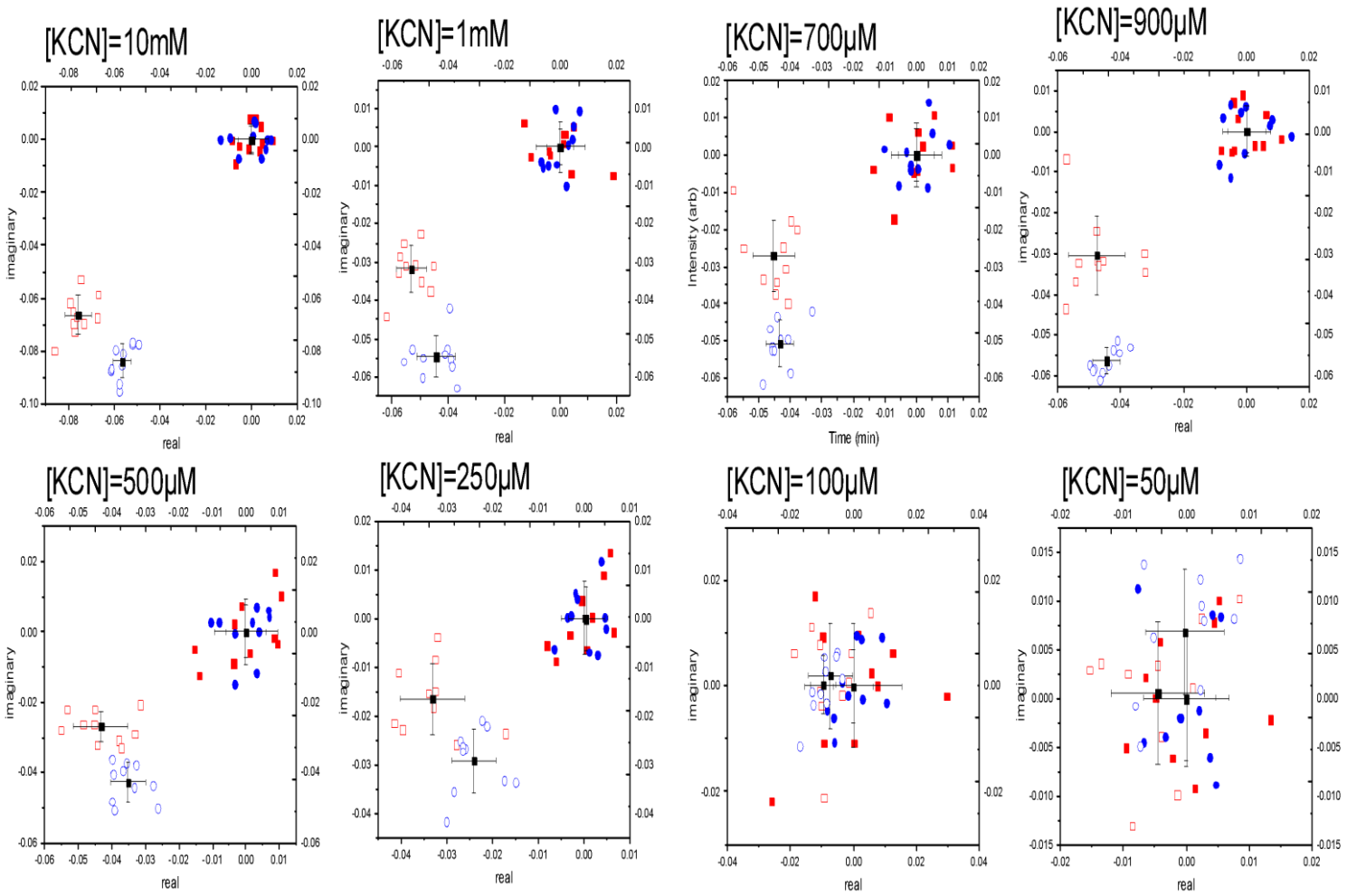


Spectral phasor plots for different concentration of cyanide added. In all figures, full gate data are blue circles, and late-gate data are red squares. Each data point is a spectrally integrated intensity versus time, normalized to the intensity prior to chemical addition (Cyanide). Filled symbols are before cyanide addition and open symbols are after cyanide addition. Similarly, figures are shown on the (top) for addition of 10mM, 1mM, 900µM and 700µM cyanide. On the bottom, 500µM, 250µM, 100µM, and 50µM of cyanide.

# KCN

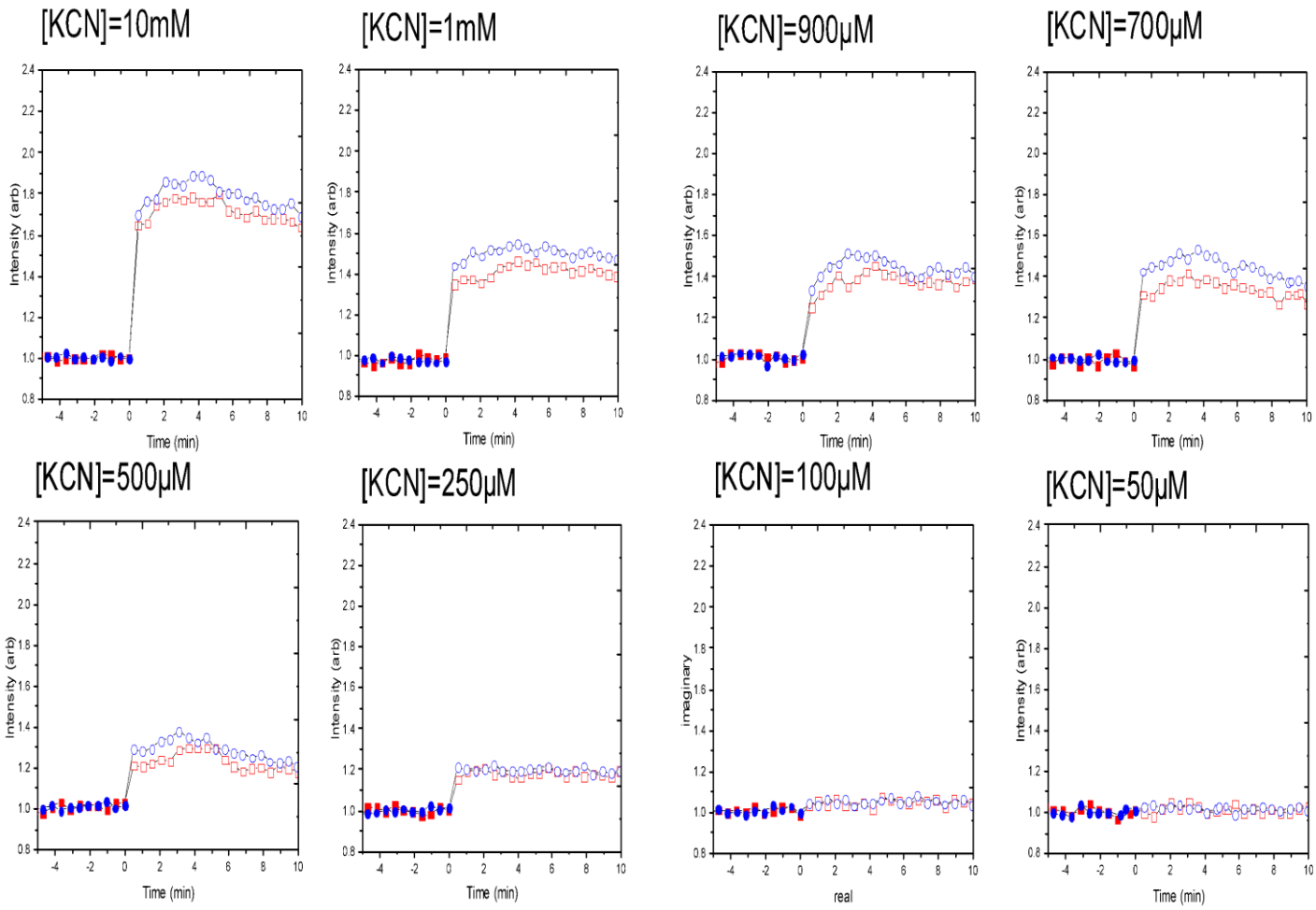


Monitoring autofluorescence response to cyanide additions. In all figures, full gate data are blue circles, and late-gate data are red squares. Each data point is a spectrally integrated intensity versus time, normalized to the intensity prior to chemical addition (Cyanide). Filled symbols are before cyanide addition and open symbols are after cyanide addition. Similarly, figures are shown on the (top) for addition of 10mM, 1mM, 900µM and 700µM cyanide. On the bottom, 500µM, 250µM, 100µM, and 50µM of cyanide.

# KCN

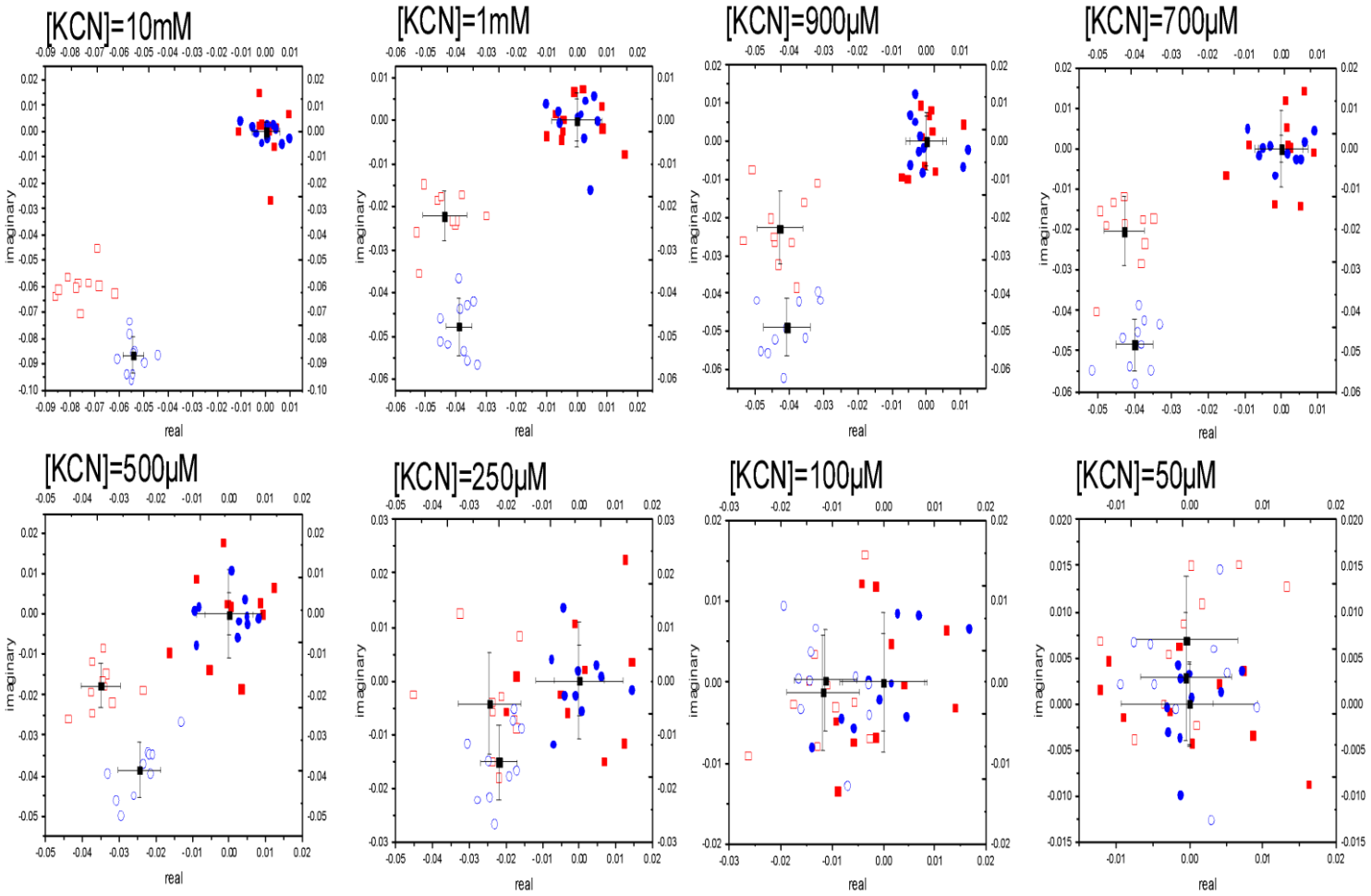


Spectral phasor plots for different concentration of cyanide added. In all figures, full gate data are blue circles, and late-gate data are red squares. Each data point is a spectrally integrated intensity versus time, normalized to the intensity prior to chemical addition (Cyanide). Filled symbols are before cyanide addition and open symbols are after cyanide addition. Similarly, figures are shown on the (top) for addition of 10mM, 1mM, 900µM and 700µM cyanide. On the bottom, 500µM, 250µM, 100µM, and 50µM of cyanide.

# Glucose+ KCN

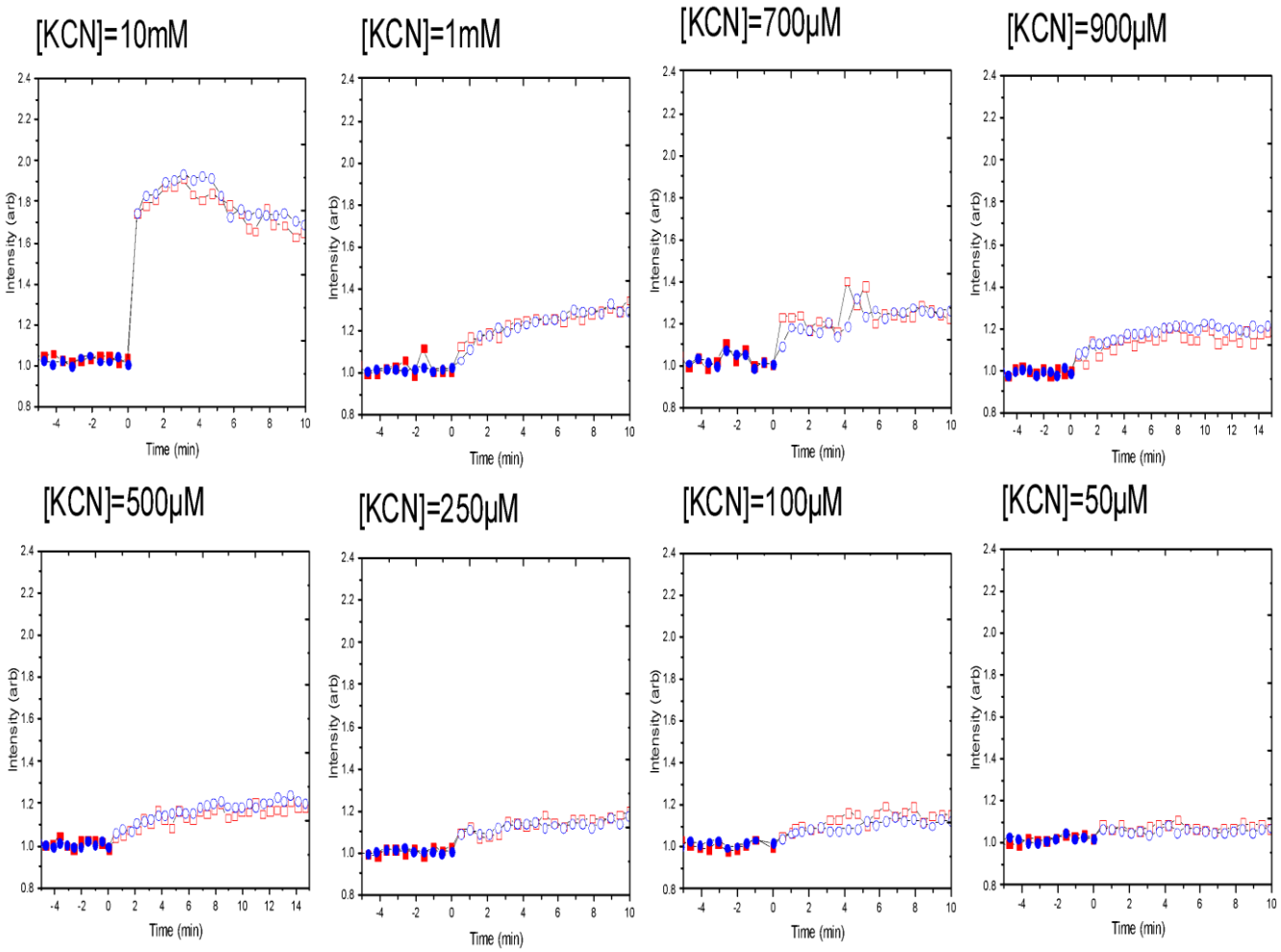


Monitoring autofluorescence response to D-glucose and cyanide additions. In all figures, full gate data are blue circles, and late-gate data are red squares. Each data point is a spectrally integrated intensity versus time, normalized to the intensity prior to chemical addition (Cyanide). Filled symbols are before cyanide addition and open symbols are after cyanide addition. Similarly, figures are shown on the (top) for addition of 10mM, 1mM, 900µM and 700µM cyanide. On the bottom, 500µM, 250µM, 100µM, and 50µM of cyanide. In all experiments, 3mM D-glucose was added 15mins prior to adding cyanide.

# Glucose+ KCN

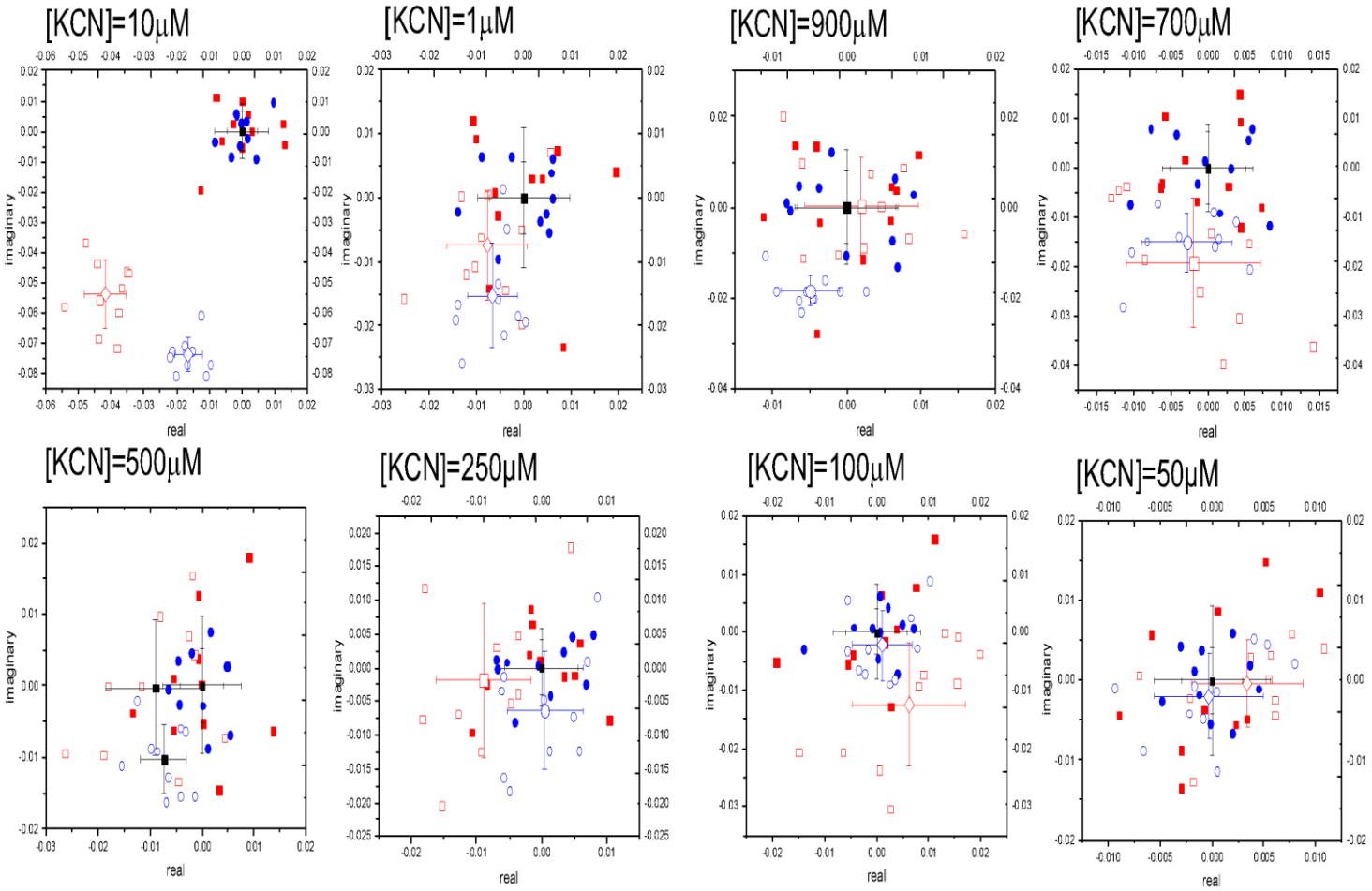


Spectral phasor plots for different concentration to D-glucose and cyanide added. In all figures, full gate data are blue circles, and late-gate data are red squares. Each data point is a spectrally integrated intensity versus time, normalized to the intensity prior to chemical addition (Cyanide). Filled symbols are before cyanide addition and open symbols are after cyanide addition. Similarly, figures are shown on the (top) for addition of 10mM, 1mM, 900µM and 700µM cyanide. On the bottom, 500µM, 250µM, 100µM, and 50µM of cyanide. In all experiments, 3mM D-glucose was added 15mins prior to adding cyanide.

# Glucose+ KCN

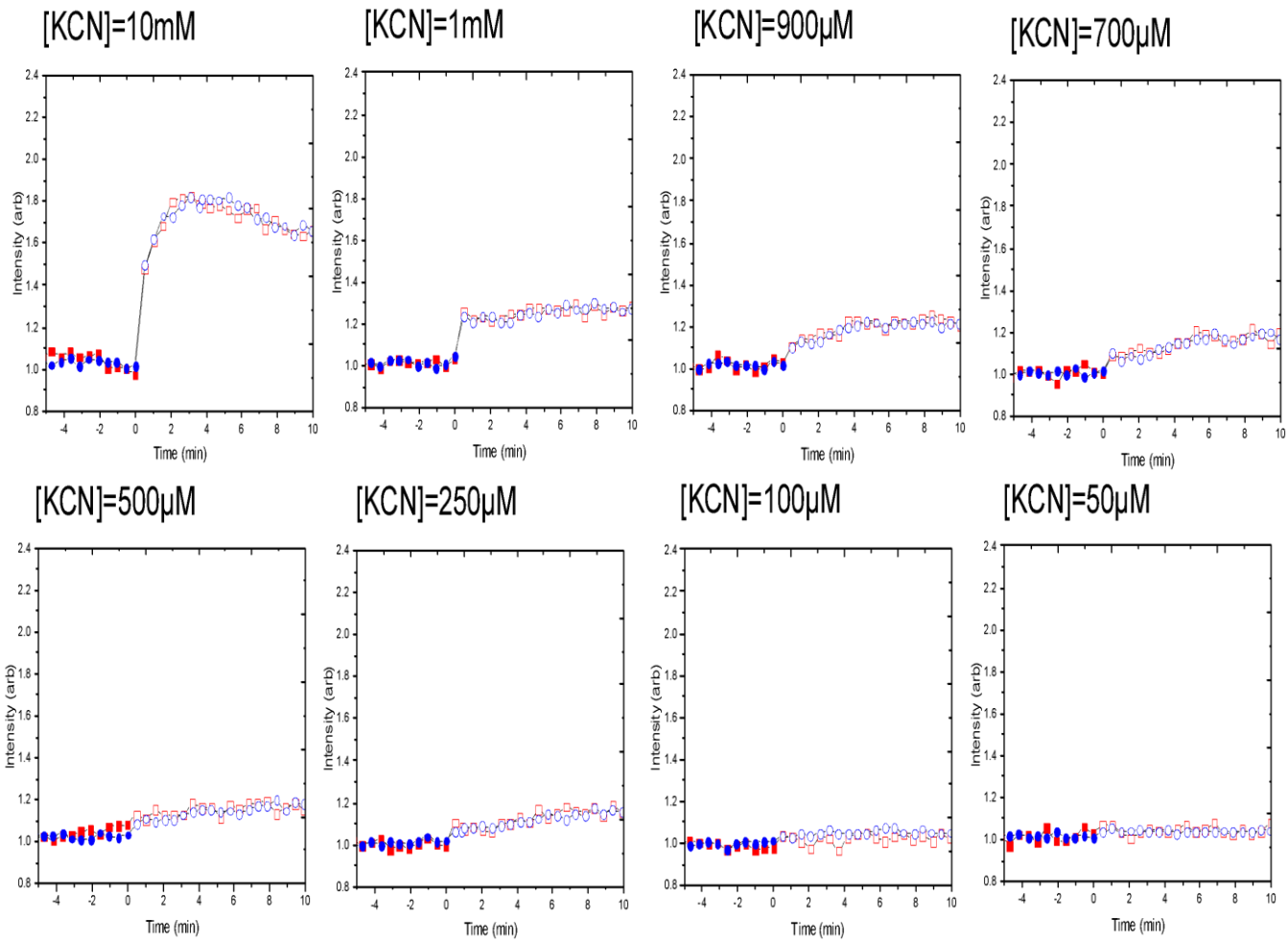


Monitoring autofluorescence response to D-glucose and cyanide additions. In all figures, full gate data are blue circles, and late-gate data are red squares. Each data point is a spectrally integrated intensity versus time, normalized to the intensity prior to chemical addition (Cyanide). Filled symbols are before cyanide addition and open symbols are after cyanide addition. Similarly, figures are shown on the (top) for addition of 10mM, 1mM, 900µM and 700µM cyanide. On the bottom, 500µM, 250µM, 100µM, and 50µM of cyanide. In all experiments, 3mM D-glucose was added 15mins prior to adding cyanide.

# Glucose+ KCN

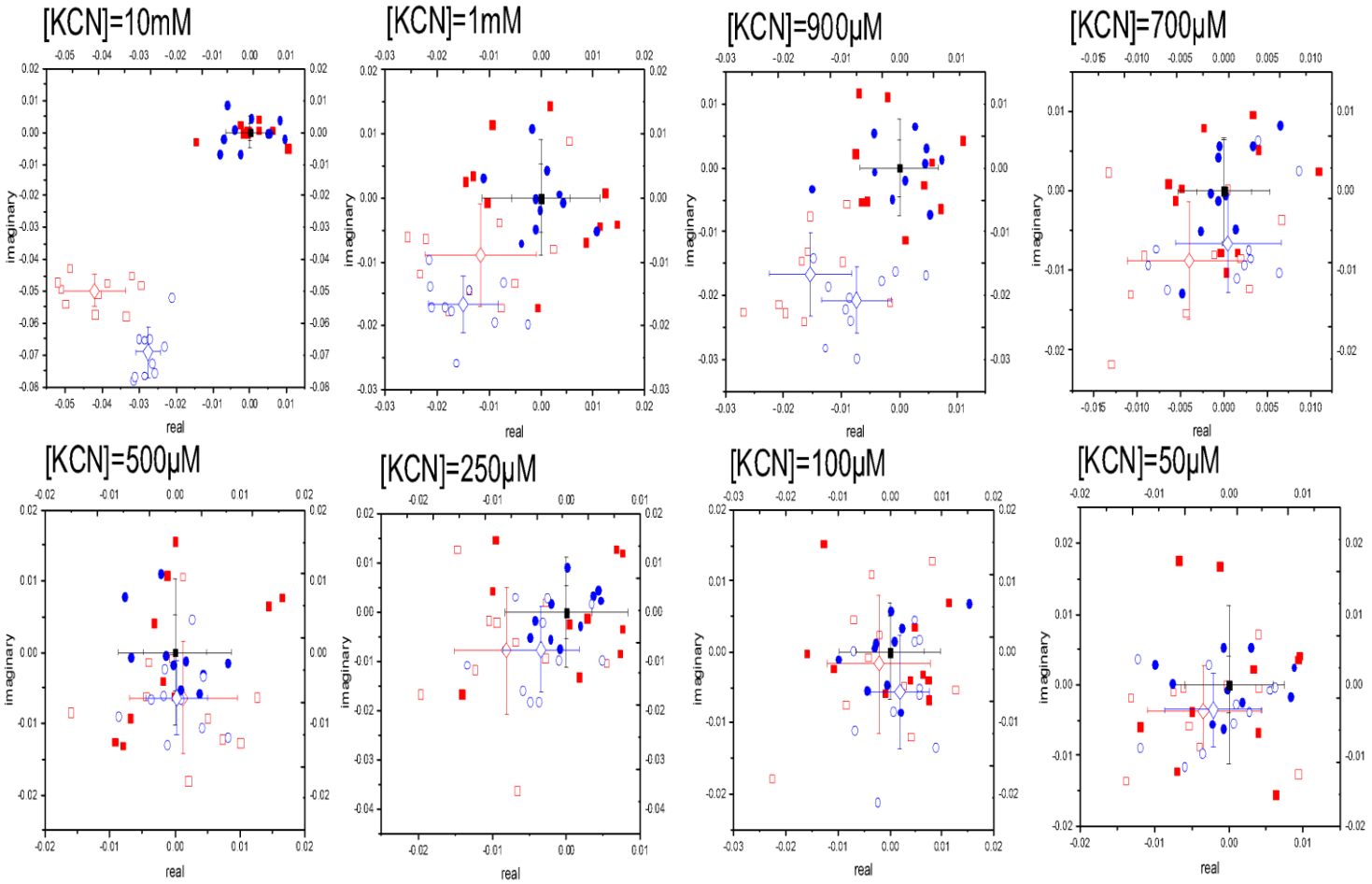


Spectral phasor plots for different concentration to D-glucose and cyanide added. In all figures, full gate data are blue circles, and late-gate data are red squares. Each data point is a spectrally integrated intensity versus time, normalized to the intensity prior to chemical addition (Cyanide). Filled symbols are before cyanide addition and open symbols are after cyanide addition. Similarly, figures are shown on the (top) for addition of 10mM, 1mM, 900µM and 700µM cyanide. On the bottom, 500µM, 250µM, 100µM, and 50µM of cyanide. In all experiments, 3mM D-glucose was added 15mins prior to adding cyanide.

# Glucose+ KCN

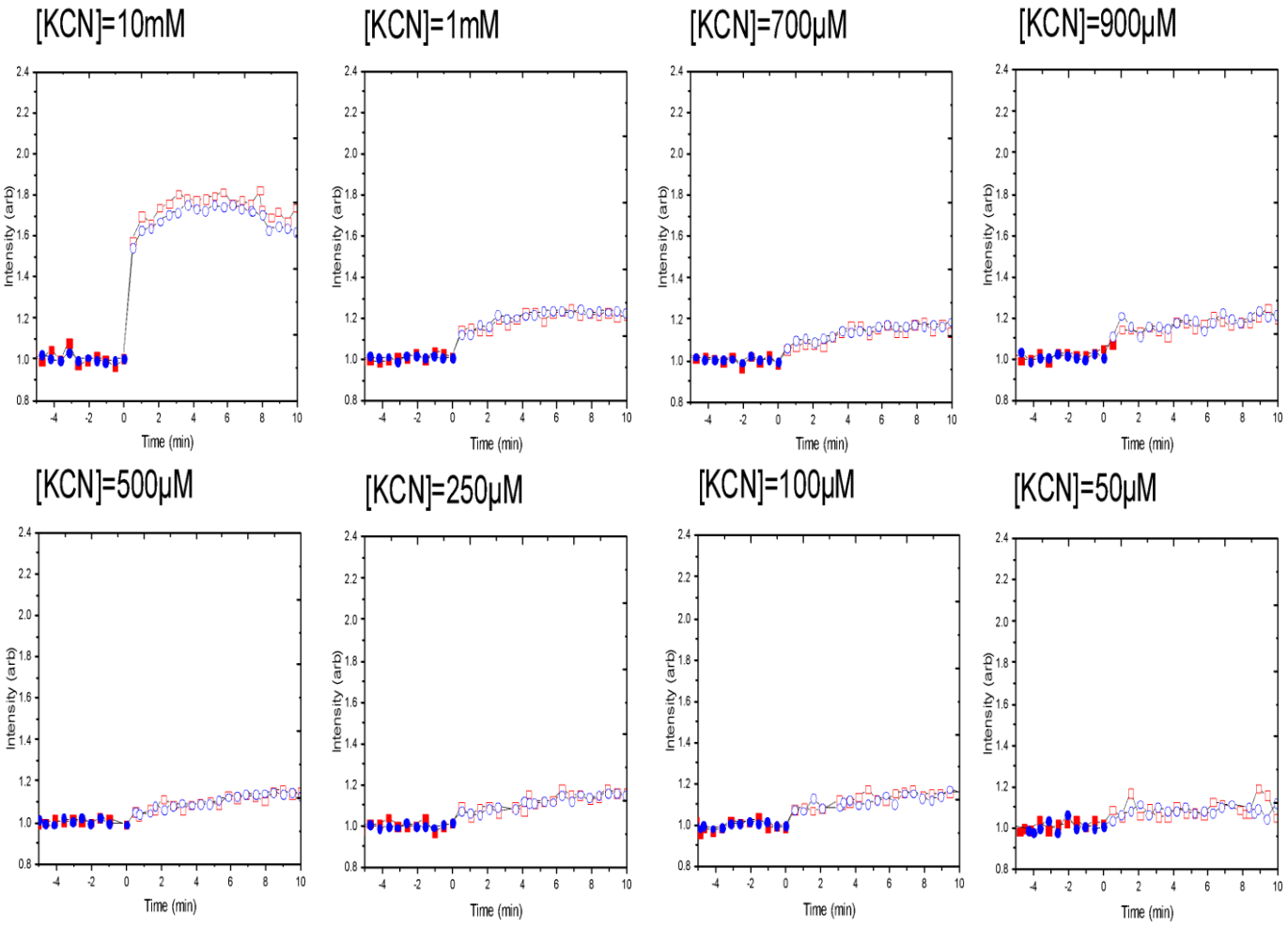


Monitoring autofluorescence response to D-glucose and cyanide additions. In all figures, full gate data are blue circles, and late-gate data are red squares. Each data point is a spectrally integrated intensity versus time, normalized to the intensity prior to chemical addition (Cyanide). Filled symbols are before cyanide addition and open symbols are after cyanide addition. Similarly, figures are shown on the (top) for addition of 10mM, 1mM, 900µM and 700µM cyanide. On the bottom, 500µM, 250µM, 100µM, and 50µM of cyanide. In all experiments, 3mM D-glucose was added 15mins prior to adding cyanide.

# Glucose+ KCN

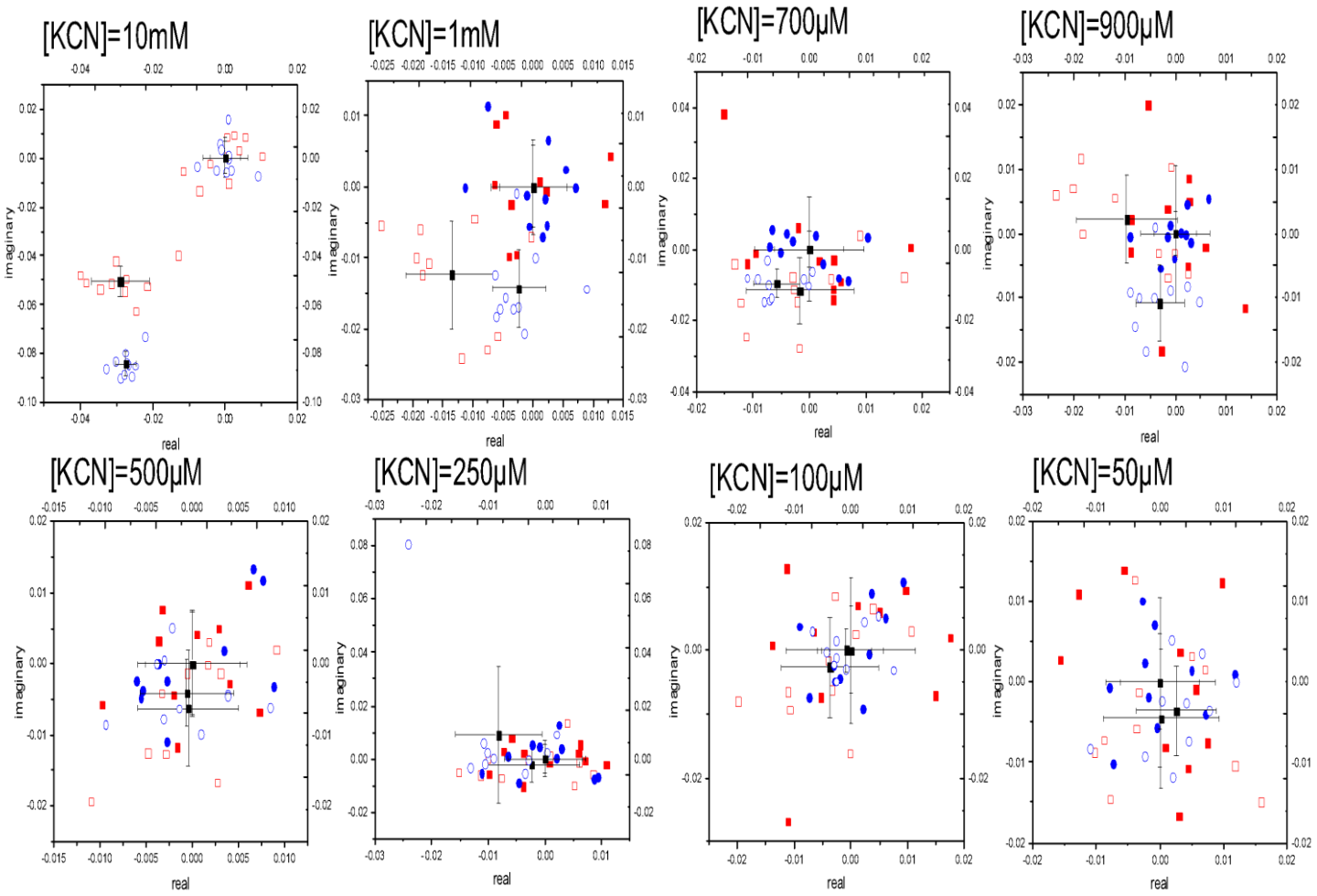


Spectral phasor plots for different concentration to D-glucose and cyanide added. In all figures, full gate data are blue circles, and late-gate data are red squares. Each data point is a spectrally integrated intensity versus time, normalized to the intensity prior to chemical addition (Cyanide). Filled symbols are before cyanide addition and open symbols are after cyanide addition. Similarly, figures are shown on the (top) for addition of 10mM, 1mM, 900µM and 700µM cyanide. On the bottom, 500µM, 250µM, 100µM, and 50µM of cyanide. In all experiments, 3mM D-glucose was added 15mins prior to adding cyanide.

# Glucose+ KCN

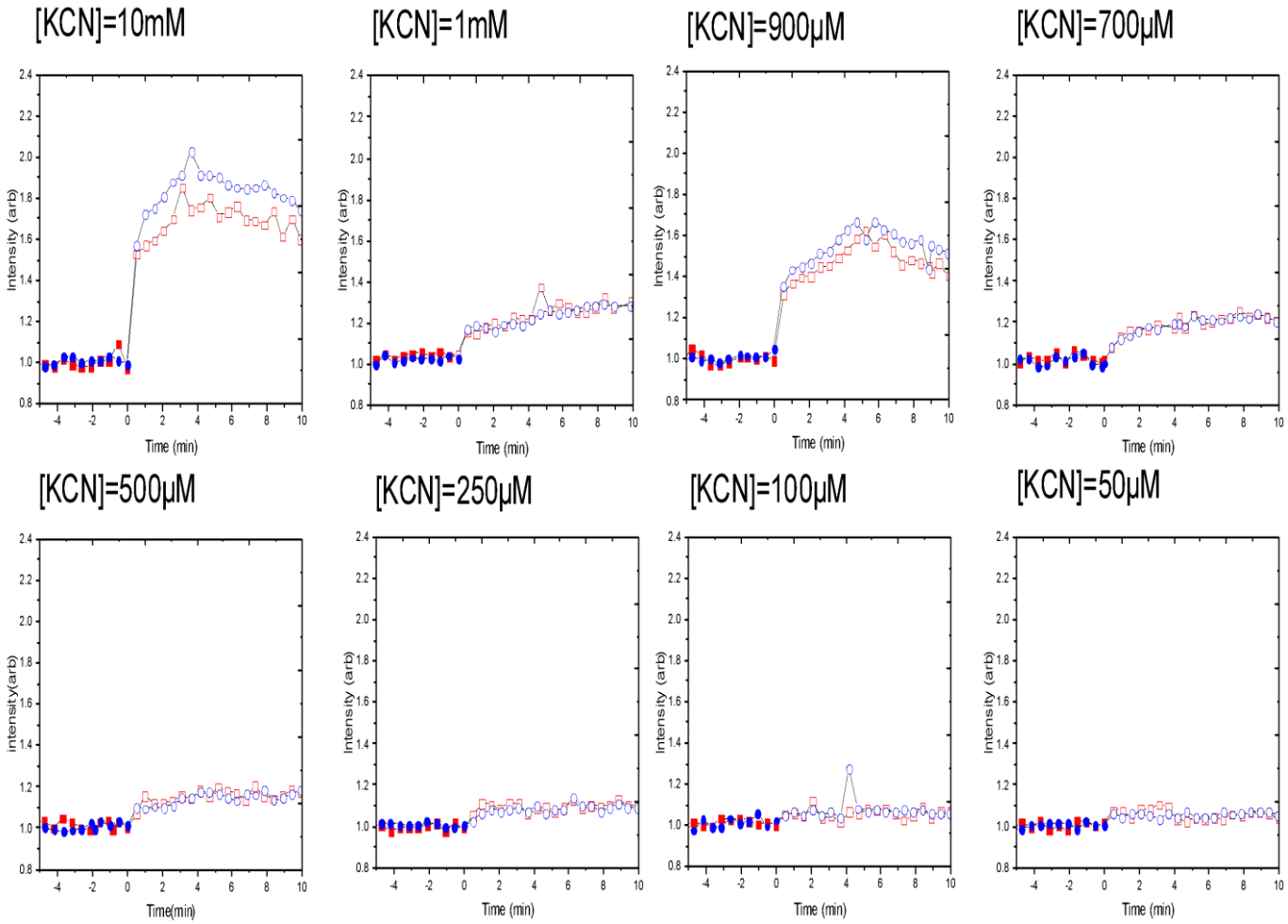


Monitoring autofluorescence response to D-glucose and cyanide additions. In all figures, full gate data are blue circles, and late-gate data are red squares. Each data point is a spectrally integrated intensity versus time, normalized to the intensity prior to chemical addition (Cyanide). Filled symbols are before cyanide addition and open symbols are after cyanide addition. Similarly, figures are shown on the (top) for addition of 10mM, 1mM, 900µM and 700µM cyanide. On the bottom, 500µM, 250µM, 100µM, and 50µM of cyanide. In all experiments, 3mM D-glucose was added 15mins prior to adding cyanide.

# Glucose+ KCN

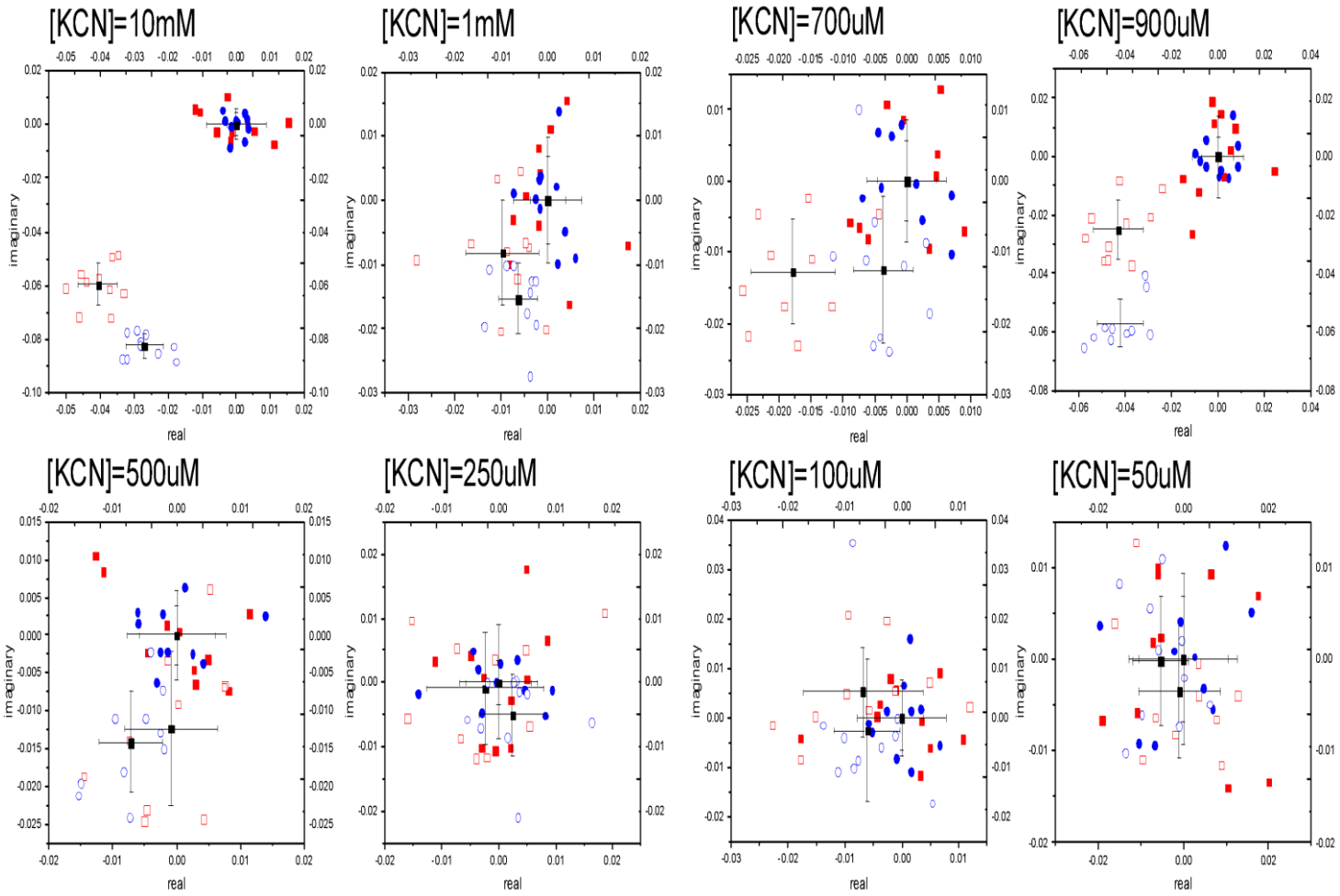


Spectral phasor plots for different concentration to D-glucose and cyanide added. In all figures, full gate data are blue circles, and late-gate data are red squares. Each data point is a spectrally integrated intensity versus time, normalized to the intensity prior to chemical addition (Cyanide). Filled symbols are before cyanide addition and open symbols are after cyanide addition. Similarly, figures are shown on the (top) for addition of 10mM, 1mM, 900µM and 700µM cyanide. On the bottom, 500µM, 250µM, 100µM, and 50µM of cyanide. In all experiments, 3mM D-glucose was added 15mins prior to adding cyanide.